NACA

RESEARCH MEMORANDUM

RELATIONSHIP OF FLOW OVER A 45° SWEPTBACK WING WITH

AND WITHOUT LEADING-EDGE CHORD-EXTENSIONS TO

LONGITUDINAL STABILITY CHARACTERISTICS

AT MACH NUMBERS FROM 0.60 TO 1.03

By F. E. West, Jr., and James H. Henderson

Langley Aeronautical Laboratory
Langley Field, Va.

NATIONAL ADVISORY COMMITTEE
FOR AERONAUTICS

WASHINGTON

October 21, 1953

3 1176 01438 0100

NATIONAL ADVISORY COMMITTEE FOR AERONAUTICS

RESEARCH MEMORANDUM

RELATIONSHIP OF FLOW OVER A 45° SWEPTBACK WING WITH

AND WITHOUT LEADING-EDGE CHORD-EXTENSIONS TO

LONGITUDINAL STABILITY CHARACTERISTICS

AT MACH NUMBERS FROM 0.60 TO 1.03

By F. E. West, Jr., and James H. Henderson

SUMMARY

Chordwise pressure distributions, tuft and ink-flow patterns, shadowgraph surveys, and force data have been obtained for a sweptback wing-fuselage combination with and without leading-edge chord-extensions. The data were obtained in the Langley 16-foot transonic tunnel at Mach numbers from 0.60 to 1.03. The wing had 45° sweep, aspect ratio of 4, taper ratio of 0.6, and NACA 65A006 airfoil sections.

An analysis of the results is presented to provide a study of the effect of leading-edge chord-extensions on the flow phenomena existing over the wing and of the relationship of these flow phenomena to the longitudinal stability characteristics of the wing. The study indicates that for Mach numbers up to 0.80 an upper-surface leading-edge separation vortex is primarily responsible for undesirable longitudinal stability characteristics. At higher Mach numbers, flow separation induced by shocks causes undesirable longitudinal stability characteristics. These undesirable characteristics are usually improved by adding chord-extensions to the wing primarily because vortices from the inboard ends of the chord-extensions act as barriers to the outboard movement of boundary-layer disturbances.

INTRODUCTION

Results of investigations of sweptback wings designed for transonic speeds have indicated undesirable longitudinal stability characteristics at both low (ref. 1) and transonic (ref. 2) speeds. Generally these wings have thin airfoil sections and small leading-edge radii and their longitudinal stability characteristics are improved by the addition to

the wings of chordwise fences or various leading-edge devices such as chord-extensions, flaps, or slats (refs. 3 to 8).

The flow phenomena responsible for these undesirable characteristics and the effect of chordwise fences and leading-edge devices on these flow phenomena have been discussed for low speeds (refs. 9 to 11). A rather detailed study of the flow phenomena existing over a sweptback wing at high subsonic and transonic speeds has been presented in reference 12.

The primary purposes of this paper are to present a study of the effect of leading-edge chord-extensions on the flow phenomena existing over a 6-percent-thick, 45° sweptback wing at high subsonic and transonic speeds and of the relationship of these flow phenomena to the longitudinal stability characteristics of the wing. The study is based on chordwise pressure distributions, tuft and ink-flow studies which indicate the flow in the boundary layer, shadowgraph surveys, and force data.

SYMBOLS

M free-stream Mach number

R Reynolds number based on $\bar{c}$

q free-stream dynamic pressure

p local static pressure

p_0 free-stream static pressure

P pressure coefficient, $\dfrac{p - p_0}{q}$

P_{cr} critical pressure coefficient

S wing area (basic wing)

b wing span

b_1 spanwise location of inboard end of chord-extension

c local basic-wing chord

$\bar{c}$ basic-wing mean aerodynamic chord

α   angle of attack of fuselage center line relative to test section center line

δ_E angle of leading-edge chord-extension chord line relative to local basic-wing chord line (positive value indicates droop)

C_L lift coefficient, $\dfrac{\text{Lift}}{qS}$

C_m pitching-moment coefficient about $0.25\bar{c}$, $\dfrac{\text{Pitching moment}}{qS\bar{c}}$

Subscripts:

B   basic model

E   model with leading-edge chord-extension

APPARATUS AND METHODS

Tunnel.- The Langley 16-foot transonic tunnel which is a single-return, octagonal, slotted-throat wind tunnel is described in reference 13.

Model.- The geometric details of the basic-model configurations and of the various leading-edge chord-extensions are shown in figure 1. This model was also used for the investigations reported in references 6, 14, and 15.

The wings and fuselage were constructed of steel and magnesium, respectively. Airfoil section ordinates may be found in reference 16. The wing was designed to have no incidence, dihedral, or twist and was mounted in a midwing position on the fuselage.

The chord-extensions at zero droop angle had the same section ordinates back to their point of maximum thickness as the corresponding spanwise wing airfoil sections. When the droop angle was not zero the ordinates were slightly modified to maintain a smooth fairing in the vicinity of the intersection between the extension chord line and the wing chord line. Between the maximum thickness points of the leading-edge chord-extensions and the wing, the airfoil contour was parallel to the wing chord line. The chord-extensions were fabricated of steel back to the 14-percent basic-wing chord line (the chord line about which the extensions were drooped), and plastic was used to continue the fairing to about the 40-percent basic-wing chord line (maximum thickness of the wing).

Usually the model was tested with the quarter chord of the wing mean aerodynamic chord located at the same longitudinal position as the maximum fuselage diameter. This configuration known as the "wing-normal configuration" is shown mounted in the test section in figure 2. However, tests were also made of a wing-aft configuration which was accomplished by shifting the fuselage forward so that the quarter chord of the mean aerodynamic chord was located $1.197\bar{c}$ to the rear of the maximum fuselage diameter. The sting sleeve which was used for the basic wing-aft configuration (see fig. 1) was not used for the wing-aft configuration with the leading-edge chord-extensions.

Support system.- The model support system was arranged so that the model was located near the center of the tunnel at all angles of attack and has been described in reference 14.

Instrumentation.- Pressure measurements were obtained over seven spanwise stations of the left wing (see fig. 1). The pressure-orifice distribution at each station which was identical on the upper and lower surfaces is given in figure 1 for the basic wing. When chord-extensions were added to the wing, pressure orifices were not available forward of 15 percent of the basic-wing chord on the four outboard spanwise stations. The pressures were transmitted by means of small tubing through the model support system to mercury manometer boards.

For the purpose of obtaining tuft and ink-flow surveys, cameras and a mercury-vapor light source were mounted in a position which enabled plan-view photographs to be taken of the wing. The wing was painted white to provide good contrast for tuft and ink-flow pictures. Tufts were made of black nylon and glued to the wing. In order to obtain ink-flow pictures, a mixture of Prussian blue and varsol was emitted from orifices located along the 5-percent chord line of the basic wing at spanwise stations of 30, 47, 64, and 75 percent of the wing semispan for the chord-extension configurations and at seven spanwise stations for the basic-wing configuration. The use of the high intensity localized light source also made it possible to employ the shadowgraph technique to show shocks on some of the tuft and ink-flow pictures. Side-view shadowgraph pictures were obtained with another camera and light source located so that the tunnel-wall flat opposite the left wing served as a shadowgraph screen.

Test conditions.- Data for the chord-extension configurations were obtained during the investigation reported in reference 6. For the basic-model configurations, force and pressure data were obtained during the investigation reported in references 14 and 15, respectively, and tuft and ink-flow surveys were obtained in a separate investigation. Data were generally obtained at Mach numbers from 0.60 to 1.03 and the tests were usually run by keeping Mach number constant and varying angle of attack. During ink-flow surveys, fresh ink was emitted continuously as the angle of attack was increased at a steady rate.

Figure 3 shows the variation of Reynolds number with Mach number for the basic-model and chord-extension configurations. The range of the Reynolds number at each Mach number is due to changes in tunnel stagnation temperature.

The pressure data and tuft, ink-flow, and shadowgraph pictures for the chord-extension configurations were not all obtained simultaneously for a given configuration. Pressure data and side-view shadowgraph pictures were obtained for one chord-extension configuration ($0.15c$, $b_1 = 0.65b/2$, $\delta_E = 0°$, wing-normal configuration); tuft pictures were obtained for another chord-extension configuration ($0.20c$, $b_1 \doteq 0.70b/2$, $\delta_E = 2.2°$, wing-normal configuration); and ink-flow pictures were obtained for another chord-extension configuration ($0.20c$, $b_1 = 0.70b/2$, $\delta_E = 0.4°$, wing-aft configuration).

RESULTS AND DISCUSSION

Some of the results from previously published papers are included in the present paper to aid the discussion. The force data for the chord-extension configurations were obtained from reference 6. For the basic-model configuration, force data were presented in reference 14, and most of the chordwise pressure-distribution data were taken from reference 15. For high lift coefficients basic model pitching-moment data were obtained from reference 2. The model used for the investigation reported in reference 2 was geometrically similar but one-third the size of the basic model used in the Langley 16-foot transonic-tunnel tests.

The data presented in this paper have not been corrected for boundary-interference effects since the results of reference 17 indicate that these effects would be small. Hence, the presented results are essentially the same as would be obtained if the model configurations were investigated in free air. Although the data showing the effect of chord-extensions have been obtained for several different configurations, the changes in configuration are not usually sufficiently large to affect a qualitative analysis of the data. Therefore, the effect of varying chord-extension configuration will be discussed only when it is considered of significance.

As indicated in reference 12, the flow phenomena existing over swept-back wings is not the same at all Mach numbers. For sweptback wing-fuselage configurations similar to those discussed in reference 12 and this paper, the general flow phenomena occurring at low speeds (ref. 9) seem to exist up to Mach numbers of about 0.80, and at higher Mach numbers shocks seem to have a predominant effect on the flow. However, at the intermediate Mach numbers (from about 0.85 to 0.94) the shock patterns

on the wing are more complicated and inducive to flow separation over
larger areas of the wing than they are at the higher Mach numbers (from
about 0.98 to 1.03). The pitching-moment curves presented in figures 4
and 5 reflect these changes in the flow phenomena. For instance, the
abruptness and magnitude of the changes in the basic model pitching-
moment curves are more severe at the intermediate Mach numbers than at
the lower and higher Mach numbers. The effects of these different flow
phenomena are also apparent in the chordwise pressure distributions shown
in figure 6 for the wing-normal configuration with and without chord-
extensions for Mach numbers from 0.60 to 1.03. For convenience the flow
phenomena for each Mach number range will usually be discussed separately.

<center>Mach Numbers up to 0.80</center>

For the wing-fuselage configuration discussed in this paper and
similar configurations it appears that for Mach numbers up to 0.80 unde-
sirable longitudinal stability characteristics exist primarily because
of the detrimental effects of a leading-edge separation vortex on the
upper-surface flow.

Flow phenomena on sweptback wings and their effect on pitching-
moment characteristics.- The mechanics of the leading-edge separation
vortex on a sweptback wing have been studied at low speeds and reported
in references 9 and 18. In reference 11 a detailed discussion is pre-
sented of the effect of the low-speed phenomena on pitching-moment char-
acteristics and of how this effect is alleviated by adding fences or
various leading-edge devices to the wing. References 19 and 12 indicate
that a leading-edge separation vortex existed on the upper surface along
the wing span at moderate angles of attack for Mach numbers of 0.60
and 0.80, respectively.

For the present investigation, the chordwise pressure distributions
at Mach numbers of 0.60 and 0.80 (figs. 6(a) and 6(b)) indicate the
presence of a leading-edge separation vortex on the basic wing at angles
of attack of 6° $\left(C_L \approx 0.4\right)$ and 8° $\left(C_L \approx 0.55\right)$ by showing a reduction of
the upper-surface pressure peaks and a broadening in the vicinity of the
leading edge of the upper-surface low-pressure region with outboard pro-
gression. These changes in the pressure distributions initially occur
at higher angles of attack and are less pronounced than shown in refer-
ence 9, probably because the wing discussed in reference 9 had a sharp
leading edge while the wing used in the present investigation had a
leading edge with a small radius. Tuft pictures shown for the basic
model at Mach numbers of 0.60 (figs. 7 and 8) and 0.80 (fig. 8) also
indicate the presence of the leading-edge separation vortex by showing
outflow along the leading-edge region at an angle of attack of 8°. The
effect of the vortex at angles of attack of 6° and 8° causes increases
in the lift over the outboard wing sections (see fig. 6) which result in

greater basic model stability for Mach numbers of 0.60 and 0.80 at lift coefficients of 0.4 or slightly higher (see figs. 4 and 5). At an angle of attack of 12° $\left(C_L \approx 0.74\right)$, regions of nearly constant pressure indicate pronounced flow separation on the outboard sections and there is a broadening of the upper-surface leading-edge pressure region over the inboard sections (fig. 6). In figure 7, the near normal direction of the tufts with respect to the free-stream direction also indicate flow separation on the outboard sections at an angle of attack of 12°. These flow changes indicate that the vortex core has turned chordwise at some outboard station and the result is a decrease of lift over the outboard sections and an increase of lift over the inboard sections. The changes are reflected in the basic-model pitching-moment curves of figures 4 and 5 which show a decrease in stability at lift coefficients of 0.6 or higher.

With further increase in angle of attack flow separation gradually progressed inboard from the tip sections (fig. 6). The increases in stability at high lift coefficients (figs. 4 and 5) occur after flow separation extends over most of the wing surface. The tuft pattern in figure 7 for the basic model at an angle of attack of 23.5° $\left(C_L = 0.93\right)$ shows that at the high lift coefficients there is an inboard flow along the leading-edge region and outboard flow along the trailing-edge region. This circulatory motion is associated with the pressure gradient that extends from the wing root to the wing tip (such as that shown in figure 6(a) at an angle of attack of 20°). A similar circulatory motion occurred at all other Mach numbers for high angle-of-attack conditions. The boundary-layer flow at high lift coefficients is complicated and cannot be suitably analyzed with available tuft pictures. However, the pictures do indicate that the flow patterns on this wing at the high lift coefficients for a Mach number of 0.60 are probably similar to those described in reference 18 for a low-speed case.

The reason that at moderate angles of attack the leading-edge separation vortex increased in chordwise extent as it moved outboard on the wing may be associated with the two-dimensional-flow characteristics of the wing airfoil section. Reference 20 shows that at low speeds the chordwise extent of a separation bubble formed near the leading edge on the upper surface of two-dimensional airfoils increased with increasing angle of attack for an airfoil that had a thickness ratio of 6 percent and for an airfoil that had a sharp leading edge. Since for a sweptback wing the effective section angle of attack increases with progression outboard until the tip sections are approached, the chordwise extent of the separation vortex would be expected to increase with outboard movement for the sharp-nosed wing discussed in reference 9 and for the thin wing of the present investigation. Reference 20 also shows that for airfoils having thickness ratios of 9 percent and 12 percent the chordwise extent of the separation bubble decreased with increasing angle of

attack. Hence, in contrast to the results of reference 9, reference 18
shows that the chordwise extent of the separation vortex decreased with
outboard movement for a sweptback wing having airfoil sections of 10 per-
cent thickness ratios. Other factors also affect the chordwise extent
of the vortex as it moves spanwise. For instance, dead air which drains
from inboard wing sections and gradually accumulates inside the vortex
as it moves outboard may affect the chordwise extent of the vortex.

Effect of chord-extensions on flow phenomena and pitching-moment
characteristics.- Studies at low speeds (ref. 11) indicate that for a
lifting condition, the plan-form discontinuity at the inboard end of a
chord-extension gives rise to a vortex (see ref. 11) which develops in
essentially the downstream direction. This vortex turns the leading-
edge separation vortex in the downstream direction, and the direction
of rotation of the two vortices are opposite. Hence, the leading-edge
separation vortex does not extend to the outboard wing sections in the
vicinity of the leading edge. The chord-extensions may also have an
effect on the leading-edge separation vortex because of a staggering of
the chordwise pressure distributions at their inboard ends and because
the breaks in the wing surface at their inboard ends act as physical
barriers to flow movement in the outboard direction.

At Mach numbers of 0.60 and 0.80 the action of leading-edge chord-
extensions appears to be similar to that described above for the low-
speed condition. The pressure distributions of figures 6(a) and 6(b)
show that chord-extensions do not cause much change in the pressure-
distribution patterns inboard of the chord-extensions. However, the
trends of the incomplete pressure distributions for the chord-extension
configuration indicate that the leading-edge separation vortex found on
the basic wing no longer exists over the forward regions of the outboard
wing stations. These trends are substantiated by the tuft pictures for
Mach numbers of 0.60 and 0.80 in figures 7 and 8, respectively, and by
the ink-flow pictures for a Mach number of 0.60 in figure 9. In addition
the pressure distributions (figs. 6(a) and 6(b)) and the tuft pictures
(fig. 7) show that even at high angles of attack the addition of chord-
extensions to the basic model resulted in a decrease in the extent of
flow separation over the outboard sections. These changes in the flow
over the outboard sections are reflected in the pitching-moment curves
shown for the chord-extension configurations in figures 4 and 5. That
is, the increase in stability at moderate lift coefficients is alleviated
because the leading-edge separation vortex does not extend outboard and
cause an increase in lift over the outboard sections. Also instability
at high lift coefficients resulting from flow separation is delayed.

The tuft picture in figure 7 for an angle of attack of 18° shows
that inboard of the chord-extension there is a circulatory motion of the
boundary layer which indicates flow separation and is similar to that
observed on the basic model (see fig. 7, $\alpha = 23.5°$). This circulatory

motion was also observed at other Mach numbers. Study of unpublished
tuft pictures showed that at an angle of attack of 25° the circulatory
motion extended over most of the wing upper surface. At angles of attack
of 12° and 18° the tufts (see fig. 7) indicate that a separation vortex
similar to the one observed on the basic model has formed in the leading-
edge region of the chord-extension. This vortex probably helped to cause
a loss of lift at high angles of attack over the outboard sections in the
same manner as the leading-edge separation vortex did for the basic model.
Figure 9 shows that as the leading-edge separation vortex and the vortex
from the inboard end of the chord-extension move chordwise they also tend
to move outboard and this tendency to move outboard becomes stronger with
increasing angle of attack. These vortices are probably responsible for
the initial flow separation over the trailing-edge region of the outboard
sections.

Mach Numbers From 0.85 to 0.94

As speed is increased from a Mach number of 0.80 to 0.85 and higher,
there is a marked change in the flow phenomena existing over wing con-
figurations similar to those discussed in this paper. Although there
are indications that a separation vortex still exists on the wing, shocks
have a predominant influence on the flow at these higher Mach numbers.

Description of shocks.- Figures 10 and 11 are presented to aid in a
description of the various shocks that exist on the wing at transonic
speeds. In figure 10 the ink-flow picture for a Mach number of 0.88
and an angle of attack of 10° indicates the presence of two shocks in
the vicinity of the leading-edge region. The first shock is usually
located at about 2 percent of the local wing chord. The second shock
extends from the vicinity of the wing leading-edge fuselage juncture and
sweeps across the wing span at an angle to the wing leading edge which
depends on angle of attack and Mach number (see also fig. 11). The
shocks did not appear in shadowgraph pictures, probably because they
were inclined at angles to the light source that were too large to allow
them to be detectable.

The presence of the leading-edge shocks is also indicated on the
upper surface of the wing by the pressure distributions of figure 6 for
Mach numbers of 0.85 and higher. At a Mach number of 0.85, their pres-
ence is first indicated at an angle of attack of 6°, and at higher Mach
numbers they are apparent for the lowest angle-of-attack conditions pre-
sented. In cases where the pressures indicate the existence of the
shocks at a given spanwise station, there is a slight compression at
about 2 percent of the local wing chord which indicates that the first
shock is a weak oblique compression shock. Downstream of this first
compression a second compression occurs that indicates the second shock
is an oblique compression shock which is somewhat stronger than the first
shock.

In the region between the two shocks the rather slight pressure gradient may indicate a thickening of the boundary layer or perhaps the presence of a separation vortex. Motion pictures of the ink-flow patterns indicate separation between the shocks as they show that some of the fluid collected along the second shock line moves intermittently into the region between the shocks and is then swept in the outboard direction. The boundary-layer thickness must be small in the forward portion of this region as tuft pictures such as those shown in figure 8 for Mach numbers of 0.85, 0.90, and 0.94, respectively, do not indicate flow disturbance in this region until the position of the second shock is approached, that is, except for the outboard sections where there is apparently considerable thickening of the boundary layer.

Hence, it appears that a boundary-layer flow disturbance such as a separation vortex may exist in the upper-surface leading-edge region at the higher Mach numbers. The weak oblique compression shock which occurs between this flow disturbance and the laminar boundary layer immediately behind the leading edge may be caused by the deflection of the boundary layer. The second oblique compression shock may be associated with the flow turning parallel to the wing surface in a vertical plane after it passes over the rear portion of the flow disturbance existing between the two leading-edge shocks. This second shock is also associated with the change in flow direction in the lateral plane (for example, see tuft pictures in figure 8 for Mach numbers of 0.85 and higher). It should be remembered that changes such as a change in leading-edge radius may affect the flow phenomena in the leading-edge region.

In addition to the two leading-edge shocks, figures 10 and 11 also show the presence of trailing-edge shocks and of shocks extending from the fuselage (which are referred to as decelerating-flow shocks in figs. 10 and 11). In the side-view shadowgraph picture (fig. 10) the shocks appear as multiple shocks probably because they become tangent to the light source at several points along the wing span. The trailing-edge shock is an oblique shock that is the main compression shock for the wing and it is believed the shock will exist on all sweptback configurations (with or without a fuselage). Although the trailing-edge shock exists for the Mach number range under discussion, the plan-form view for a Mach number of 1.0 and an angle of attack of 4° represents one of the few conditions where the shock was sufficiently tangent to the light source to be photographically recorded over even a portion of the wing span. The third compression shown in many of the chordwise distributions of figure 6 at the higher Mach numbers indicates the presence of the trailing-edge shock.

In figure 10 for a Mach number of 0.94 and an angle of attack of 10° the shock extending from the fuselage can be traced across the fuselage, the tunnel floor, and the upper surface of the wing-tip region. This shock is first noticeable at a Mach number of 0.90 (see tuft pictures in fig. 12 at angles of attack of 6° and 8° for the chord-extension configuration) and increasing Mach number or angle of attack causes it to move downstream. A detailed discussion of the trailing-edge shock and

the shock extending from the fuselage has been presented for low angle-of-attack conditions in reference 12.

The pressure distributions for Mach numbers of 0.85, 0.90, and 0.94 (fig. 6) indicate that with movement outboard the second leading-edge shock and the trailing-edge shock gradually converge until they join at some outboard station as illustrated in figure 11. This point of juncture moves outboard and rearward with increase in Mach number. At Mach numbers of 0.90 and 0.94 the shock extending from the fuselage tends to reinforce the shocks in the wing-tip region (see fig. 11).

Flow phenomena on basic model and their effect on pitching-moment characteristics.- The pressure distributions of figure 6 show that as Mach number is increased from 0.85 to 0.94 at low lift coefficients there is a rearward shift in the center of pressure. This shift is reflected in the pitching-curves of figures 4 and 5. The pressure distributions also show that increases in stability at moderate lift coefficients $(C_L \approx 0.5)$ shown in figures 4 and 5 at intermediate Mach numbers are primarily due to the effects of boundary-layer thickening or separation causing lift increases and rearward shifts of center of pressure over the outboard sections. At higher lift coefficients the basic model becomes unstable at the intermediate Mach numbers primarily because of a loss of lift over the outboard sections, caused by the spread of flow separation (see figs. 6(c), 6(d), and 6(e)).

Although the unstable moment break is mainly a result of flow separation over the outboard sections as it also is at lower speeds, the flow separation at these higher Mach numbers is caused primarily by the detrimental effect of the shocks previously described and not by the effects of a leading-edge separation vortex.

As previously indicated, some of the shocks tend to reinforce each other over the outboard sections (see fig. 11). Thus, boundary-layer disturbances and flow separation may be expected to occur first in the outboard regions. In figures 12 and 13, the tufts indicate at an angle of attack of 6° that initial boundary-layer disturbances do occur on the outboard sections and are confined behind or in the vicinity of the shocks for both the basic model and chord-extension configurations. Also figures 6(c), 6(d), 6(e), 12, and 13 show that the flow first separates over the outboard sections. Even after separation initially occurs on the outboard sections, tufts show that boundary-layer outflow over the inboard sections is confined behind or in the vicinity of the shocks (for example, see tuft pictures for Mach numbers of 0.85, 0.90, and 0.94 in fig. 8). The shocks are probably aided in causing flow separation over the outboard sections by the tendency of the boundary layer on a sweptback wing to flow outboard and create a thickened boundary layer over the outboard sections which is rather easily separated. At higher angles of attack the shocks become stronger and eventually aid the spread of flow separation over most of the wing (see figs. 12 and 13).

The unstable pitching-moment break for the basic model (see fig. 4)
is more abrupt at a Mach number of 0.90 than at Mach numbers of 0.85
or 0.94. At lift coefficients of about 0.6 ($\alpha \approx 8^{\circ}$) the pitching-moment
coefficient is more negative for a Mach number of 0.90 than for a Mach
number of 0.85, primarily because of higher loadings over the outboard
sections (see fig. 6) at a Mach number of 0.90. Hence, because there is
not much difference in the outboard loadings or pitching-moment coeffi-
cients for the two Mach numbers at lift coefficients of about 0.71
($\alpha \approx 10^{\circ}$) or greater where extensive flow separation exists over the out-
board sections, the unstable pitching-moment break is more severe for a
Mach number of 0.90. As increasing Mach number to 0.94 causes the shocks
to become stronger and move farther downstream, flow separation occurs
initially at lower lift coefficients and spreads over the outboard sec-
tions at a slower rate with increasing lift coefficient than at the two
lower Mach numbers. These changes in the flow result in a more gradual
unstable pitching-moment slope at a Mach number of 0.94 than at a Mach
number of 0.90. Changes in the pitching-moment curves as Mach number is
increased from 0.85 to 0.94 may also be affected by a variation of wing-
fuselage interference with Mach number. The unstable pitching-moment
break at a Mach number of 0.94 becomes more abrupt when the fuselage is
moved forward on the wing (see figs. 4 and 5) because the shocks on the
wing move forward (ref. 15) and apparently have about the same effect
as the shocks on the wing-normal configuration at a Mach number of 0.90.

Effect of chord-extensions on flow phenomena and pitching-moment
characteristics.- The ink-flow patterns shown in figure 14 for a Mach
number of 0.90 are believed to be representative of boundary-layer flow
patterns that exist on the chord-extension configurations from Mach
numbers of 0.85 to 0.94. The patterns for angles of attack of 5° and 6°
show boundary-layer outflow over the inboard sections in the vicinity of
the two leading-edge shocks and in the vicinity of a shock at the mid-
chord line which is the trailing-edge shock or a combination of this
shock with the shock extending from the fuselage. (The counterclockwise
motion of the boundary layer inboard of the chord-extension shown in fig-
ure 14 for angles of attack above 6° was also observed at the lower Mach
numbers.) At spanwise stations near the inboard end of the chord-
extension the boundary-layer flow at angles of attack of 5° and 6°
(fig. 14) is turned in the downstream direction probably because the
vortex from the inboard end of the chord-extension resists outflow of
the boundary layer. The second leading-edge shock, the trailing-edge
shock, and the shock extending from the fuselage must extend across this
vortex region because outflow is indicated over the outboard sections at
chordwise positions where the shocks would be expected to lie. Pressure
distributions for the chord-extension configuration such as that shown
in figure 6(d) at 70 percent of the wing semispan for an angle of attack
of 6° also indicate that these shocks exist over the outboard sections.
However, the pressure distributions are too incomplete to determine if
the first leading-edge shock extends over the outboard sections or if
other shocks originate in the vicinity of the chord-extension leading edge.

Pressure distributions and tuft pictures for Mach numbers of 0.85 (see figs. 6 and 8) and 0.90 (see figs. 6, 8, and 12) show that adding chord-extensions to the wing resulted in an elimination or reduction of flow separation over the outboard sections. It appears that this flow improvement occurred primarily because the vortex from the inboard end of the chord-extension prevented the boundary-layer outflow created at the inboard sections from moving outboard and causing a thickened boundary layer that could be easily separated by the shocks. However, at a Mach number of 0.94, figure 6 shows that the effect of chord-extensions on flow separation and loading over the outboard sections is much less than at Mach numbers of 0.85 or 0.90. This smaller effect which is also illustrated by comparing the tuft pictures of figures 12 and 13 apparently occurred because the shocks at a Mach number of 0.94 were more inducive to flow separation over the outboard sections than the weaker shocks at Mach numbers of 0.85 and 0.90.

Study of figure 6 will indicate how the outboard loading changes caused by adding chord-extensions to the basic model alleviate the abruptness of the unstable pitching-moment breaks shown in figures 4 and 5 for the intermediate Mach numbers. Some of the alleviation shown for a Mach number of 0.94 in figure 4 may be because the chord-extensions added wing area ahead of the shock positions where unseparated flow could exist (see fig. 13). Adding chord-extensions to the wing-aft configuration provided no improvement in the pitching-moment characteristics at a Mach number of 0.94 (fig. 5) probably because the shocks moved forward on the wing when the body was moved forward and allowed flow separation to extend to the leading edges of the chord-extensions.

As leading-edge devices such as chord-extensions only partially counteract the detrimental effect of shocks at Mach numbers of 0.90 and 0.94, it would be desirable to weaken the shocks or to displace them so that they create smaller regions of separated flow. It may be possible to lessen the effect of the shocks by making changes in fuselage and wing geometry. Reference 21 shows that changes in wing geometry such as reducing thickness, and decreasing sweep will improve pitch-up characteristics. Also reducing aspect ratio will be beneficial (see ref. 22).

Mach Numbers From 0.98 to 1.03

At Mach numbers between 0.98 and 1.03 the position of the shocks over the wing have changed so that their detrimental effects on flow separation are confined to smaller regions of the wing than at the intermediate Mach numbers (see fig. 8 and ref. 12).

A rather large rearward shift in the trailing-edge shock position occurs over the outboard portion of the wing when Mach number is increased from 0.94 to 0.98 (see fig. 6, $\alpha = 4^\circ$). At a Mach number

of 0.94 the shock extending from the fuselage merges with the trailing-edge shock thus influencing the position of the trailing-edge shock over the outboard portion of the wing. However, at a Mach number of 0.98 the shock extending from the fuselage moves downstream of the wing, except at very low angles of attack, and probably allows the trailing-edge shock to seek a more rearward position. The flow over the wing leading-edge region is similar to that previously discussed for Mach numbers between 0.85 and 0.94 (see fig. 6) except that a detached bow wave exists at Mach numbers of about 1.00 and higher (see ref. 12).

Flow phenomena on basic model and their effect on pitching-moment characteristics.- The rate of increase in stability shown in figure 4 at lift coefficients of 0.40 to 0.50 for Mach numbers of 0.98 to 1.03 is less than at a Mach number of 0.94. This occurs because the shock positions over the outboard sections at low angles of attack are farther rearward at Mach numbers above 0.94 (see fig. 6), and hence, initial boundary-layer disturbances that are confined behind the shocks would tend to cause smaller changes in outboard loading distribution at the higher Mach numbers.

For angles of attack where flow separation initially occurs, separation at the higher Mach numbers is confined to a region over the outboard stations that lies behind chordwise positions where the second leading-edge shock reinforces the trailing-edge shock (see basic-model tuft picture for a Mach number of 1.00 in fig. 8). Study of unpublished tuft pictures shows that as angle of attack is increased the flow separation gradually spreads along and behind the second leading-edge shock and the trailing-edge shock and then spreads upstream of the shock positions. Since the spread of flow separation is rather gradual with increasing angle of attack the unstable pitching-moment break (fig. 4), resulting from separation causing a loss of lift initially over the outboard stations (see figs. 6(f), 6(g), and 6(h)), is not nearly as abrupt at the higher Mach numbers as at the intermediate Mach numbers.

Effect of chord-extensions on flow phenomena and pitching-moment characteristics.- Figure 4 shows that at a Mach number of 0.98 addition of chord-extensions to the basic model resulted in considerable alleviation of the pitch-up tendency. Although the pitching-moment curves for Mach numbers of 1.00 and 1.03 do not extend to very high lift coefficients, flow patterns at moderate lift coefficients for these Mach numbers are similar to those at a Mach number of 0.98, and hence chord-extensions should alleviate the pitch-up tendency at these higher Mach numbers. The pressure distributions at Mach numbers of 0.98 and 1.00 (fig. 6) show that adding chord-extensions to the wing delayed the upstream spread of flow separation over the outboard stations. Comparison of the tuft pictures in figure 8 at a Mach number of 1.00 shows that the flow disturbances in the trailing-edge region are not as severe for the chord-extension configuration as for the basic-model configuration. Hence, it

is concluded that chord-extensions alleviate the abruptness of the pitch-up tendency at the higher Mach numbers for basically the same reasons as were noted for a Mach number of 0.94.

CONCLUDING REMARKS

Results of a study of the effect of leading-edge chord-extensions on the flow phenomena existing over a 45° sweptback wing at Mach numbers from 0.60 to 1.03 and of the relationship of these flow phenomena to the longitudinal stability characteristics of the wing form the basis for the following general remarks.

At speeds up to a Mach number of 0.80 the effects of upper-surface leading-edge separation vortices are primarily responsible for undesirable pitching-moment characteristics. These undesirable pitching-moment characteristics are improved by adding chord-extensions to the wing primarily because vortices from the inboard ends of the chord-extensions act as barriers to the outward spread of separation.

At Mach numbers of 0.85 to 1.03 a weak oblique shock lies parallel to the wing leading-edge and is usually located at about 2 percent of the local wing chord. A stronger oblique shock extends from the vicinity of the wing leading-edge fuselage juncture in a lateral direction and sweeps back at a greater angle than the wing leading edge. There is evidence that a thickened boundary layer or a separation vortex lies between these two shocks.

At Mach numbers of 0.85 to 1.03 the second leading-edge shock and shocks downstream of the leading-edge shocks extend laterally across the wing and cause flow separation over the outboard wing sections which results in undesirable pitching-moment characteristics.

The forward position of shocks on the wing at Mach numbers from 0.85 to 0.94 allows them to create flow separation over large portions of the wing area which results in very undesirable pitching-moment characteristics. Vortices from the inboard ends of the chord-extensions improve the pitching-moment characteristics because they retard the boundary-layer flow created at the inboard stations from moving outboard and causing a thickened boundary layer that can be easily separated by shocks.

With increase in Mach number to 0.98 or higher the shocks move rearward on the wing and cause a reduction of the separated flow area with a resultant improvement in the pitching-moment characteristics. Chord-extensions are effective in improving pitching-moment characteristics at a Mach number of 0.98 because they add wing area in unseparated flow

regions and because their vortices have an effect similar to that noted
at Mach numbers from 0.85 to 0.94.
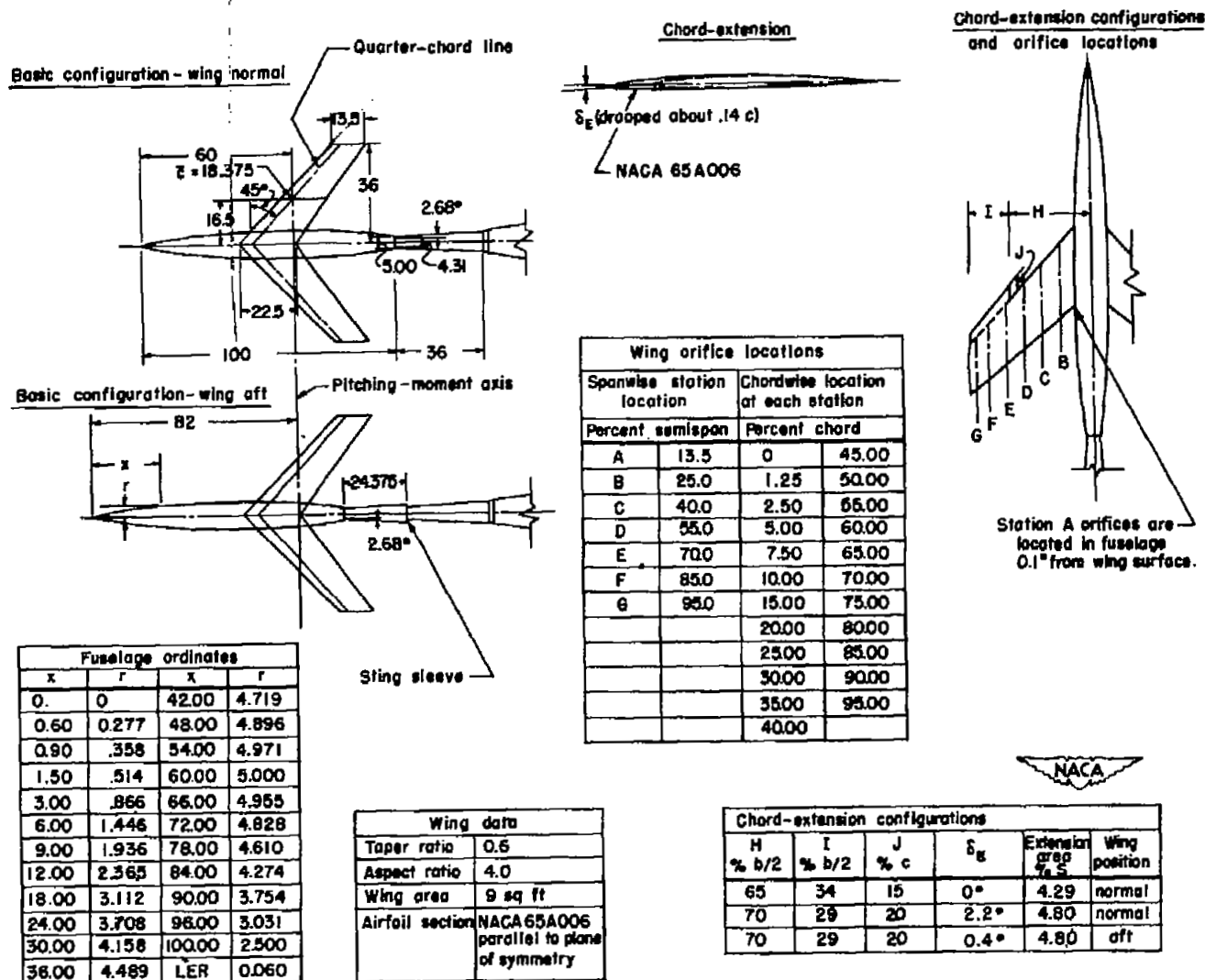

Langley Aeronautical Laboratory,
      National Advisory Committee for Aeronautics,
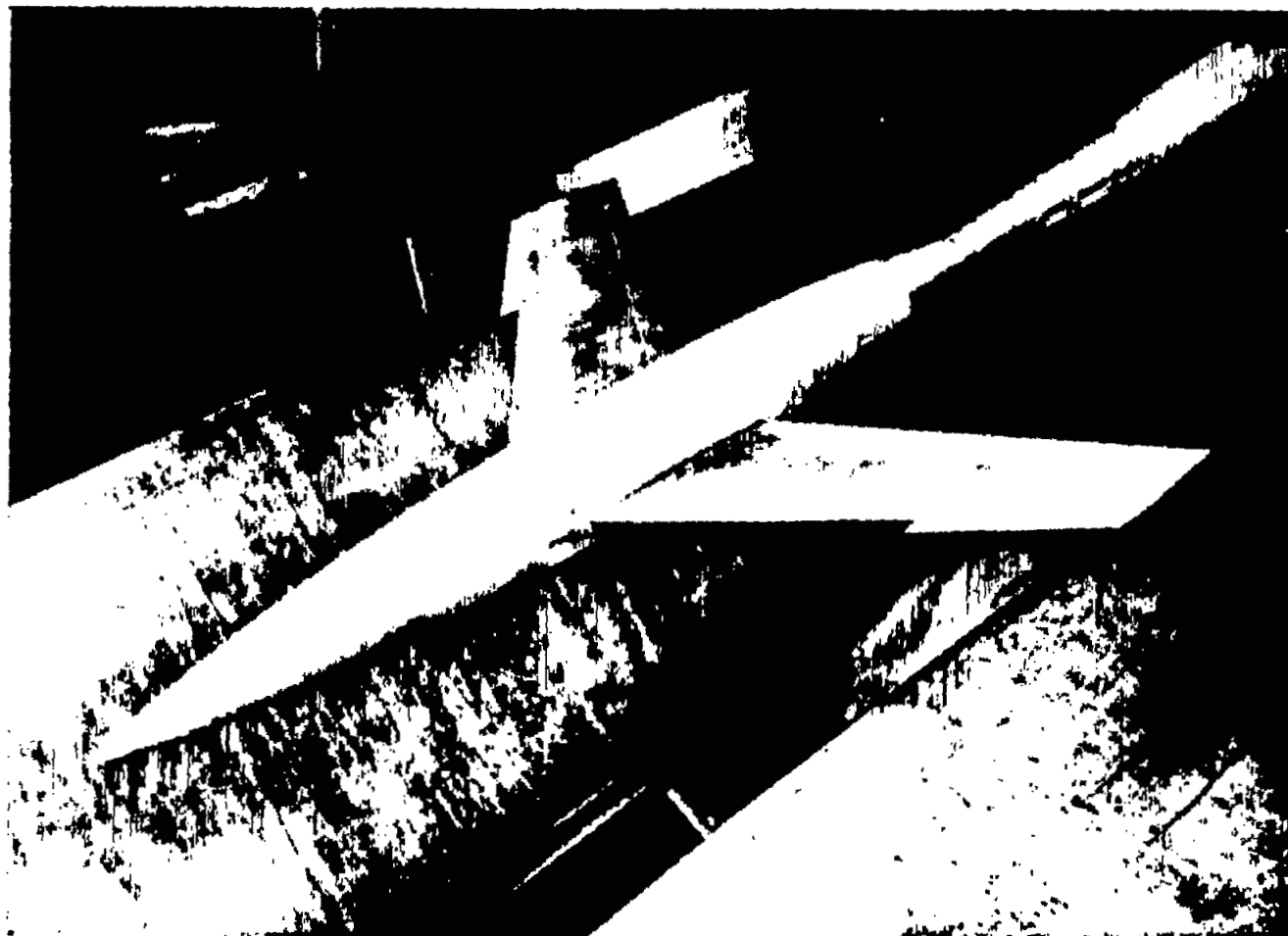   Langley Field, Va., August 11, 1953.

REFERENCES

1. Cahill, Jones F., and Gottlieb, Stanley M.: Low-Speed Aerodynamic
   Characteristics of a Series of Swept Wings Having NACA 65A006 Air-
   foil Sections (Revised). NACA RM L50F16, 1950.

2. Osborne, Robert S., and Mugler, John P., Jr.: Aerodynamic Character-
   istics of a 45° Sweptback Wing-Fuselage Combination and the Fuselage
   Alone Obtained in the Langley 8-Foot Transonic Tunnel. NACA
   RM L52E14, 1952.

3. Lowry, John G., and Schneiter, Leslie E.: Investigation at Low Speed
   of the Longitudinal Stability Characteristics of a 60° Swept-Back
   Tapered Low-Drag Wing. NACA TN 1284, 1947.

4. Hieser, Gerald: An Investigation at Transonic Speeds of the Effects
   of Fences, Drooped Nose, and Vortex Generators on the Aerodynamic
   Characteristics of a Wing-Fuselage Combination Having a 6-Percent-
   Thick, 45° Sweptback Wing. NACA RM L53B04, 1953.

5. Furlong, G. Chester: Exploratory Investigation of Leading-Edge
   Chord-Extensions To Improve the Longitudinal Stability Character-
   istics of Two 52° Sweptback Wings. NACA RM L50A30, 1950.

6. West, F. E., Jr., Liner, George, and Martz, Gladys S.: Effect of
   Leading-Edge Chord-Extensions on the Aerodynamic Characteristics
   of a 45° Sweptback Wing-Fuselage Combination at Mach Numbers of 0.40
   to 1.03. NACA RM L53B02, 1953.

7. Goodson, Kenneth W., and Few, Albert G., Jr.: Effect of Leading-Edge
   Chord-Extensions on Subsonic and Transonic Aerodynamic Character-
   istics of Three Models Having 45° Sweptback Wings of Aspect Ratio 4.
   NACA RM L52K21, 1953.

8. Runckel, Jack F., and Steinberg, Seymour: Effects of Leading-Edge
   Slats on the Aerodynamic Characteristics of a 45° Sweptback Wing-
   Fuselage Configuration at Mach Numbers of 0.40 to 1.03. NACA
   RM L53F23, 1953.

9. Lange, Roy H., Whittle, Edward F., Jr., and Fink, Marvin P.:
   Investigation at Large Scale of the Pressure Distribution and Flow
   Phenomena Over a Wing With the Leading Edge Swept Back 47.5° Having
   Circular-Arc Airfoil Sections and Equipped With Drooped-Nose and
   Plain Flaps. NACA RM L9G15, 1949.

10. Jaquet, Byron M.: Effects of Chord Discontinuities and Chordwise
    Fences on Low-Speed Static Longitudinal Stability of an Airplane
    Model Having a 35° Sweptback Wing. NACA RM L52C25, 1952.

11. Furlong, G. Chester, and McHugh, James G.: A Summary and Analysis
    of the Low-Speed Longitudinal Characteristics of Swept Wings at
    High Reynolds Number. NACA RM L52D16, 1952.

12. Whitcomb, Richard T., and Kelly, Thomas C.: A Study of the Flow
    Over a 45° Sweptback Wing-Fuselage Combination at Transonic Mach
    Numbers. NACA RM L52D01, 1952.

13. Ward, Vernon G., Whitcomb, Charles F., and Pearson, Merwin D.:
    Air-Flow and Power Characteristics of the Langley 16-Foot Transonic
    Tunnel With Slotted Test Section. NACA RM L52E01, 1952.

14. Hallissy, Joseph M., and Bowman, Donald R.: Transonic Character-
    istics of a 45° Sweptback Wing-Fuselage Combination. Effect of
    Longitudinal Wing Position and Division of Wing and Fuselage Forces
    and Moments. NACA RM L52K04, 1953.

15. Solomon, William, and Schmeer, James W.: Effect of Longitudinal Wing
    Position on the Pressure Characteristics at Transonic Speeds of a
    45° Sweptback Wing-Fuselage Model. NACA RM L52K05a, 1953.

16. Loftin, Lawrence K., Jr.: Theoretical and Experimental Data for a
    Number of NACA 6A-Series Airfoil Sections. NACA Rep. 903, 1948.
    (Supersedes NACA TN 1368.)

17. Whitcomb, Charles F., and Osborne, Robert S.: An Experimental
    Investigation of Boundary Interference on Force and Moment Char-
    acteristics of Lifting Models in the Langley 16- and 8-Foot Tran-
    sonic Tunnels. NACA RM L52L29, 1953.

18. Black, Joseph: A Note on the Vortex Patterns in the Boundary Layer
    Flow of a Swept-Back Wing. Jour. R.A.S., vol. LVI, Apr. 1952,
    pp. 279-285.

19. Loving, Donald L., and Estabrooks, Bruce B.: Transonic-Wing
    Investigation in the Langley 8-Foot High-Speed Tunnel at High
    Subsonic Mach Numbers and at a Mach Number of 1.2. Analysis of
    Pressure Distribution of Wing-Fuselage Configuration Having a Wing
    of 45° Sweepback, Aspect Ratio 4, Taper Ratio 0.6, and NACA
    65A006 Airfoil Section. NACA RM L51F07, 1951.

20. McCullough, George B., and Gault, Donald E.: Examples of Three
    Representative Types of Airfoil-Section Stall at Low Speeds.
    NACA TN 2502, 1951.

21. Donlan, Charles J., and Weil, Joseph: Characteristics of Swept Wings at High Speeds. NACA RM L52A15, 1952.

22. Kuhn, Richard E., and Wiggins, James W.: Wind-Tunnel Investigation of the Aerodynamic Characteristics in Pitch of Wing-Fuselage Combinations at High Subsonic Speeds. Aspect-Ratio Series. NACA RM L52A29, 1952.

Basic configuration - wing normal

Quarter-chord line

Chord-extension

Chord-extension configurations and orifice locations

δ_E (drooped about .14 c)

NACA 65A006

60
$\bar{c} = 18.375$
45°
16.5
36
13.5
2.68°
5.00 4.31
-22.5
100
36

Basic configuration - wing aft

Pitching-moment axis

82
x
r
24.375
2.68°

Sting sleeve

Station A orifices are located in fuselage 0.1" from wing surface.

Wing orifice locations		
Spanwise station location	Chordwise location at each station	
Percent semispan	Percent chord	
A	13.5	0	45.00
B	25.0	1.25	50.00
C	40.0	2.50	55.00
D	55.0	5.00	60.00
E	70.0	7.50	65.00
F	85.0	10.00	70.00
G	95.0	15.00	75.00
		20.00	80.00
		25.00	85.00
		30.00	90.00
		35.00	95.00
		40.00	

Fuselage ordinates			
x	r	x	r
0.	0	42.00	4.719
0.60	0.277	48.00	4.896
0.90	.358	54.00	4.971
1.50	.514	60.00	5.000
3.00	.866	66.00	4.955
6.00	1.446	72.00	4.828
9.00	1.936	78.00	4.610
12.00	2.365	84.00	4.274
18.00	3.112	90.00	3.754
24.00	3.708	96.00	3.031
30.00	4.158	100.00	2.500
36.00	4.489	LER	0.060

Wing data	
Taper ratio	0.6
Aspect ratio	4.0
Wing area	9 sq ft
Airfoil section	NACA 65A006 parallel to plane of symmetry

NACA

Chord-extension configurations					
H % b/2	I % b/2	J % c	δ_B	Extension area % S	Wing position
65	34	15	0°	4.29	normal
70	29	20	2.2°	4.80	normal
70	29	20	0.4°	4.80	aft

H
I
J
F
E
D
C
B
G

Figure 1.- Dimensions of basic model and leading-edge chord-extensions.
All dimensions are in inches.

L-73078

Figure 2.- Three-quarter view showing wing-normal configuration with
leading-edge chord-extensions (0.15c, $b_1 = 0.65b/2$, $\delta_E = 0^\circ$)
mounted in the test section.
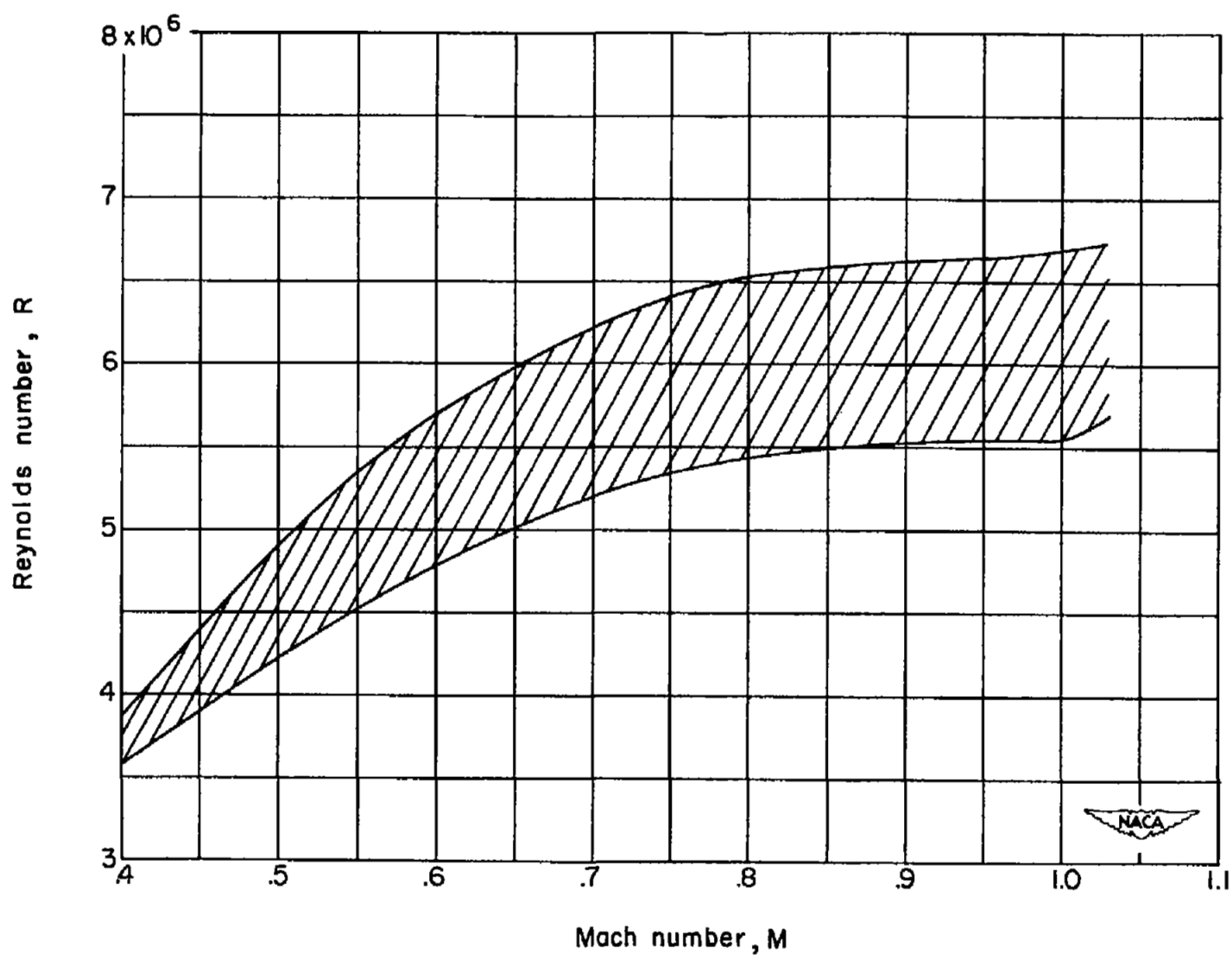
Figure 3.- Variation of Reynolds number with Mach number.
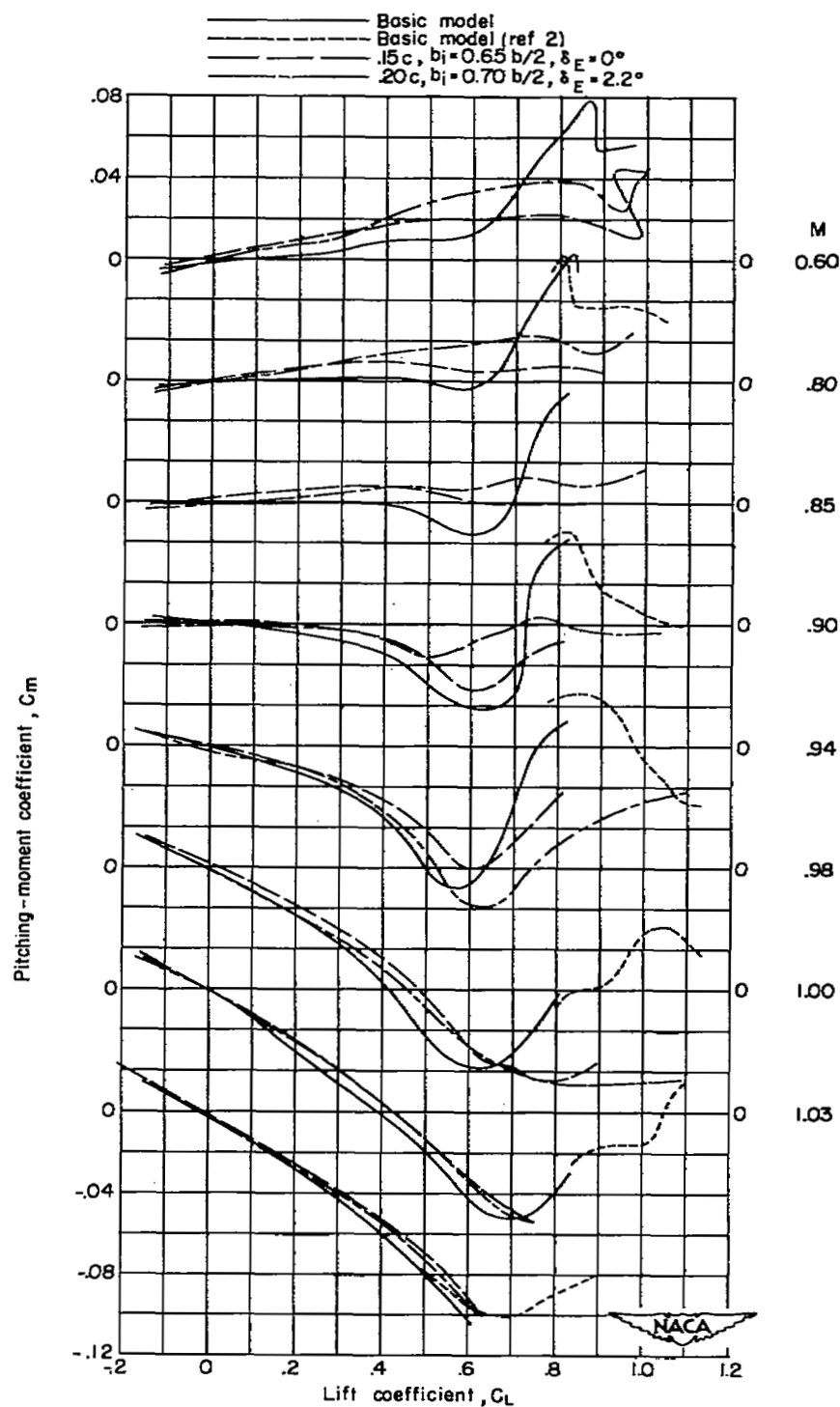
Figure 4.- Pitching-moment characteristics for basic wing-normal
configuration and for two wing-normal chord-extension configurations.
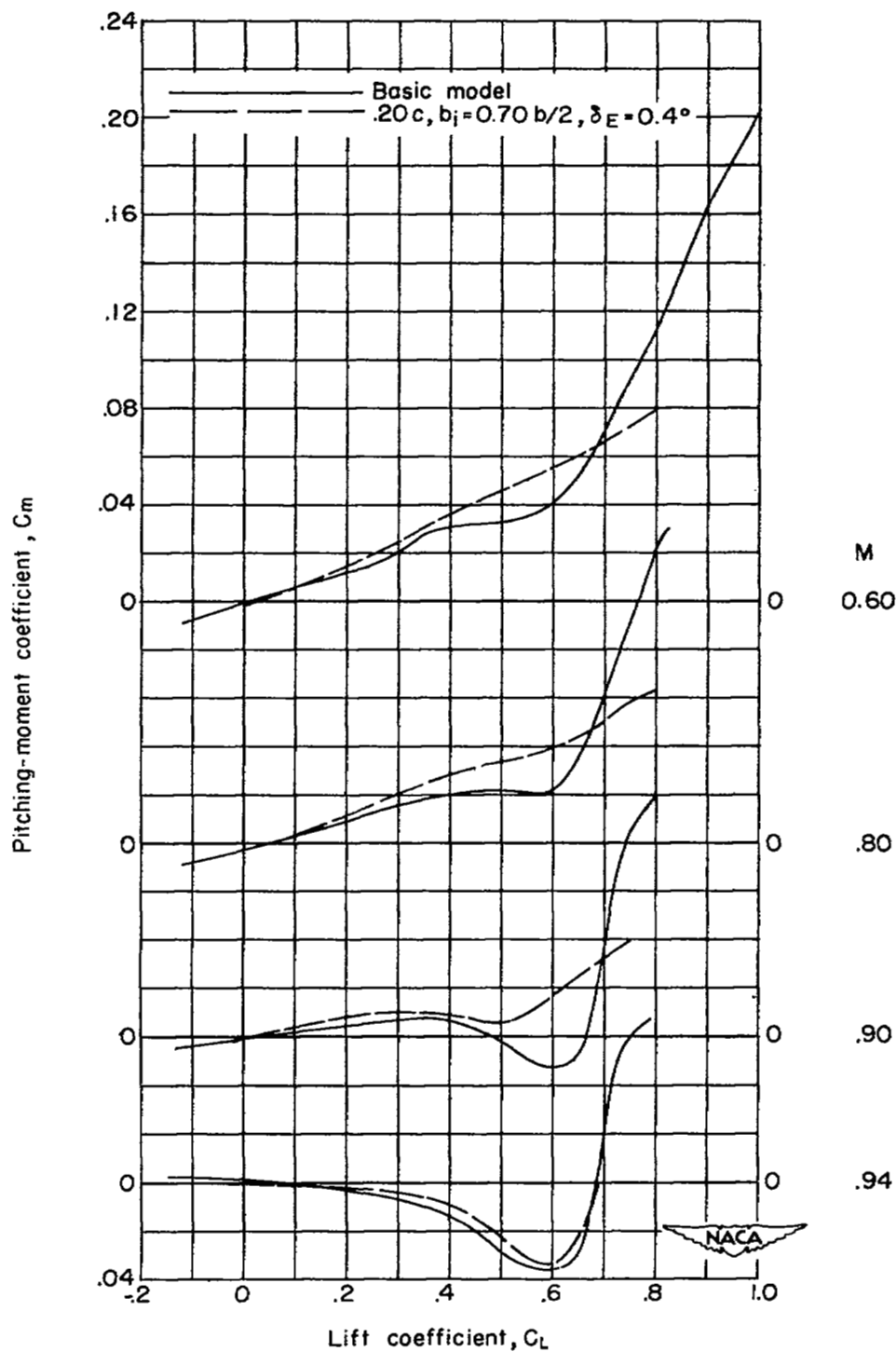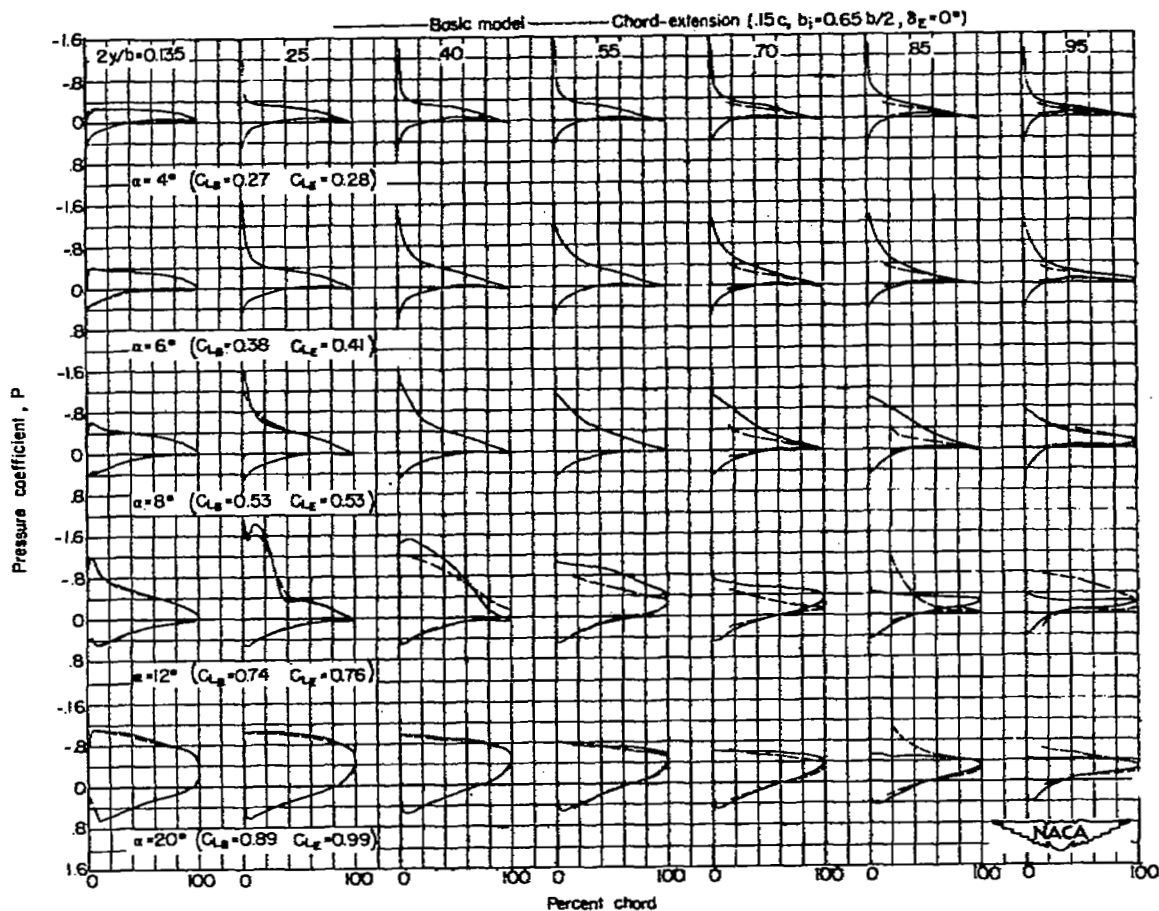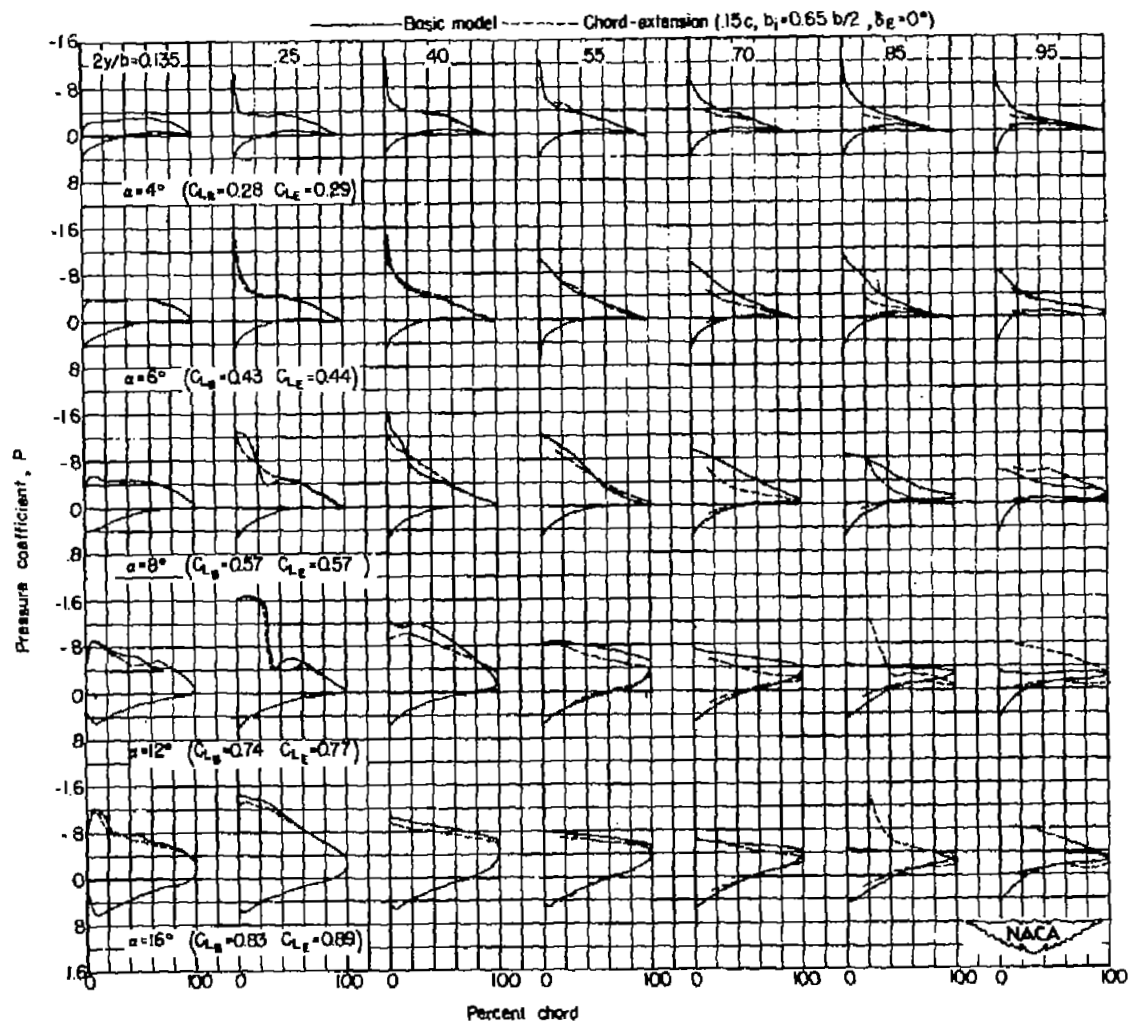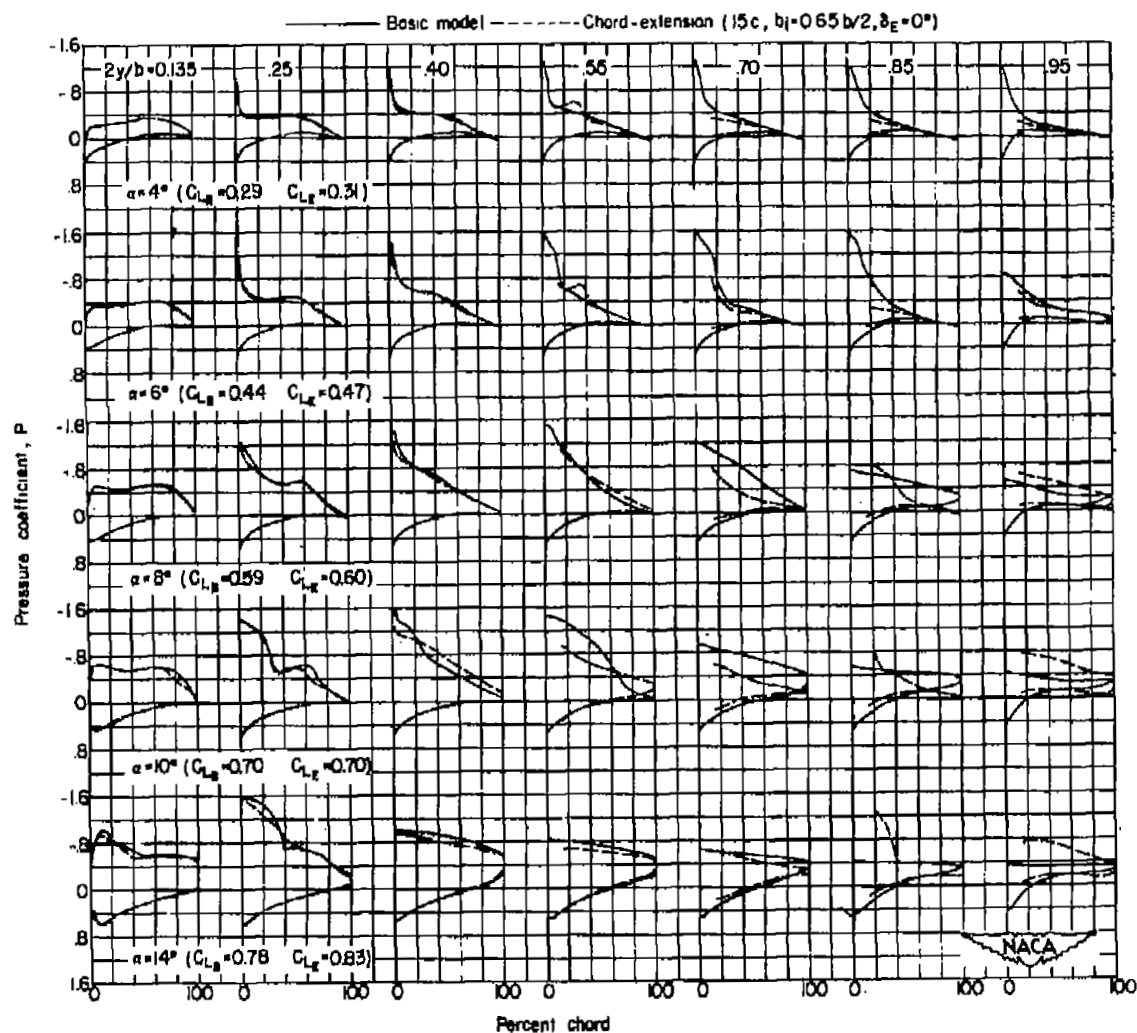
Figure 5.- Pitching-moment characteristics for basic wing-aft configuration and for a wing-aft chord-extension configuration.

(a)   M = 0.60; P_{cr} = -1.30.

Figure 6.- Chordwise pressure distributions for wing (wing-normal
configuration) with and without chord-extension.

Basic model ———— Chord-extension (.15c, b$_i$ =0.65 b/2 , δ$_E$ =0°)

(b) M = 0.80; P$_{cr}$ = -0.43.

Figure 6.- Continued.

——— Basic model ————Chord-extension (l5c , b₁=0 65 b/2, δₑ=0°)

(c)   M = 0.85; P_{cr} = -0.30.

Figure 6.- Continued.
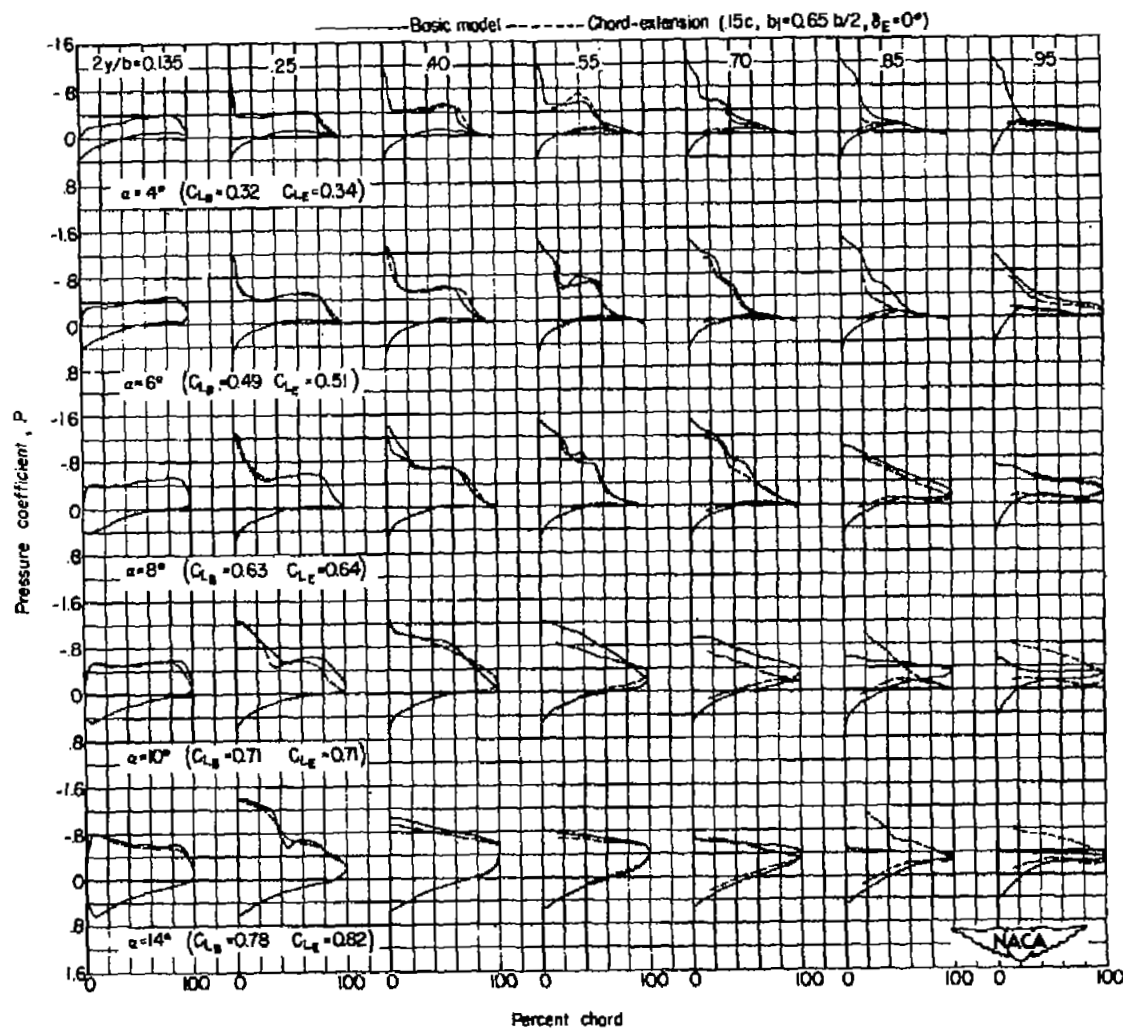
(d) $M = 0.90$; $P_{cr} = -0.19$.

Figure 6.- Continued.

Basic model ———— Chord-extension (.15c, b₁=0.65 b/2, Sₑ=0°)
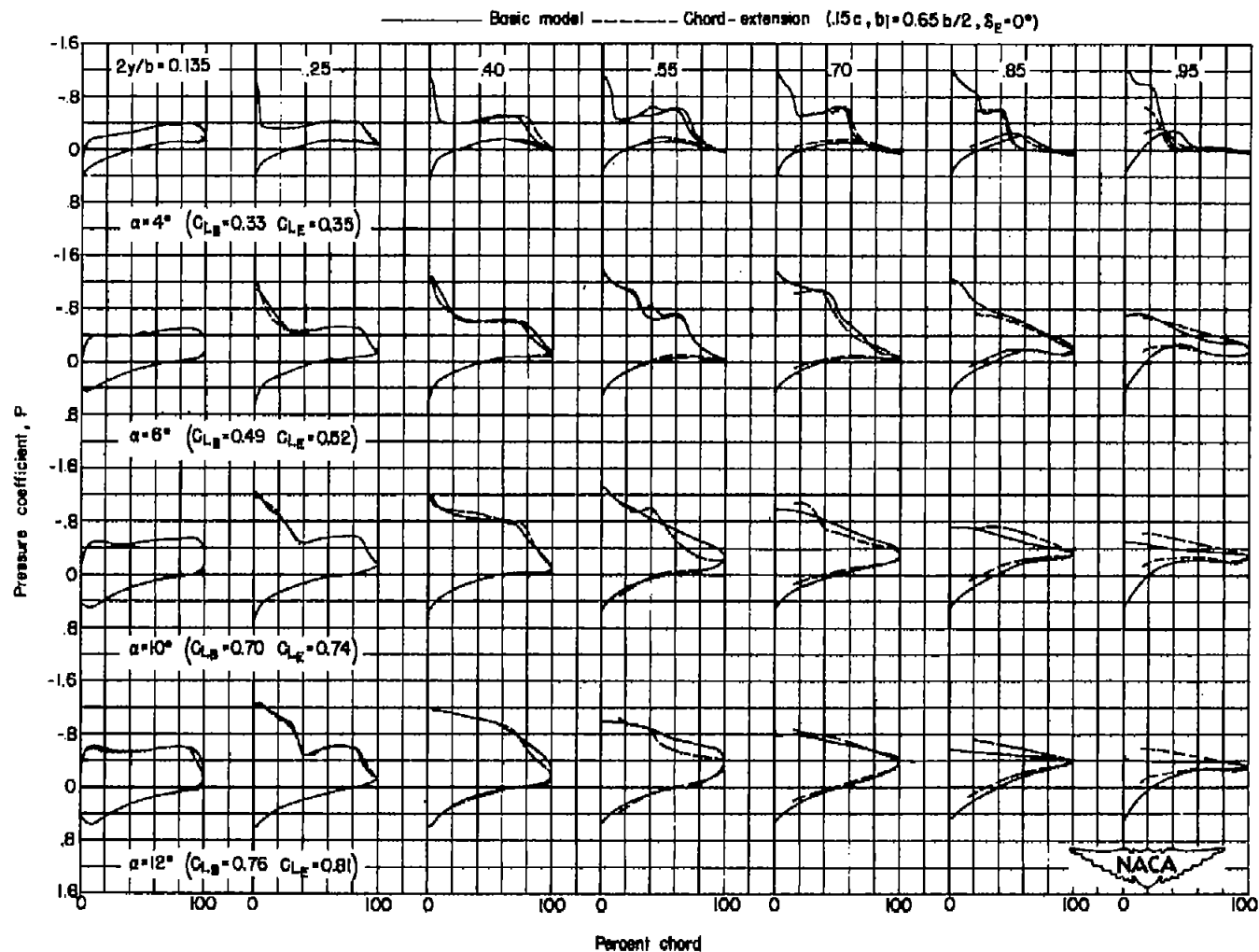
(e) M = 0.94; P_{cr} = -0.11.

Figure 6.- Continued.
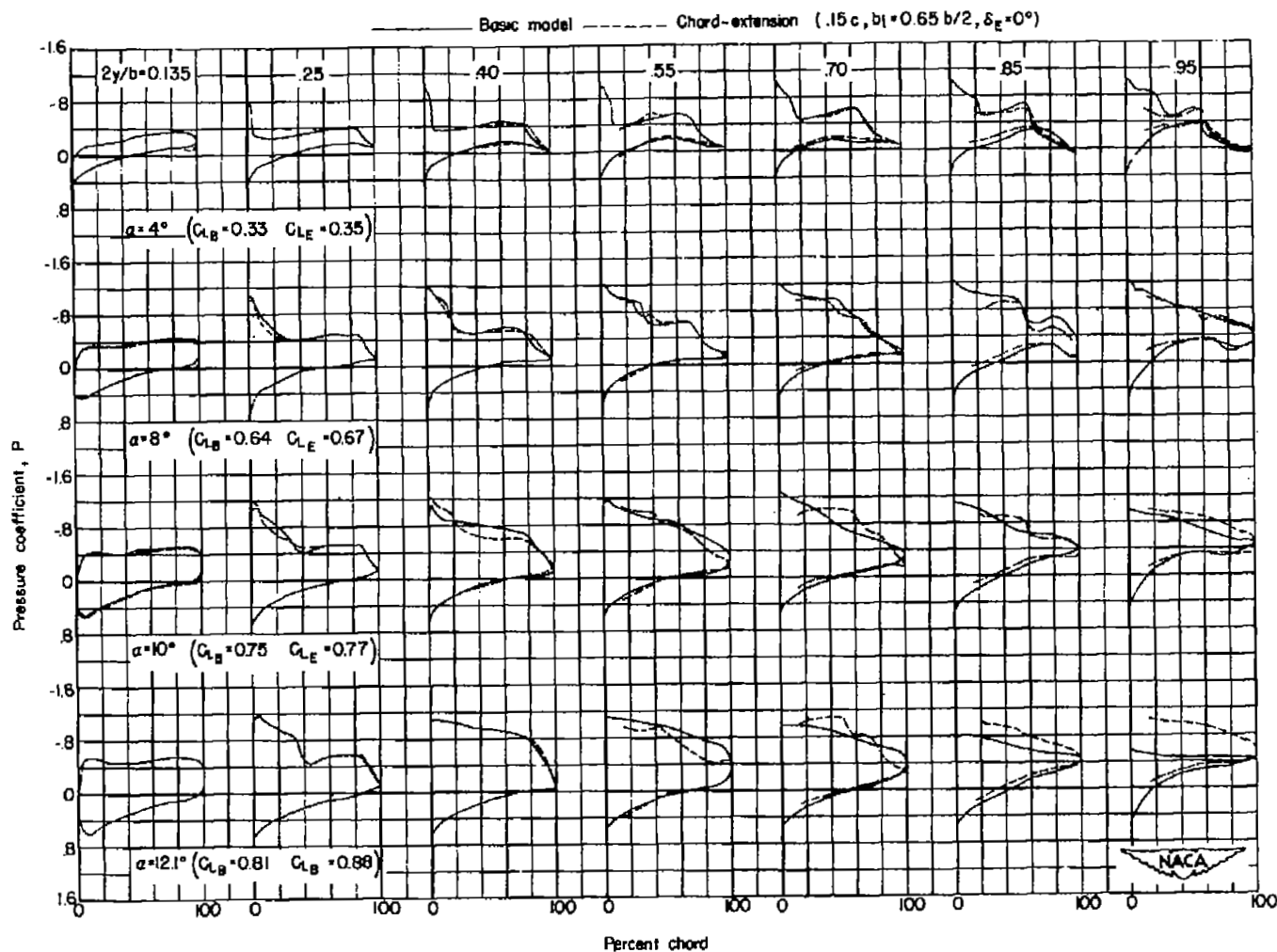
(f)   M = 0.98; P_{cr} = -0.03.

Figure 6.- Continued.

Basic model ————— Chord-extension (.15c, b$_i$=0.65 b/2, δ_E=0°)

Pressure coefficient, P

2y/b=0.135   .25   .40   .55   .70   .85   .95

a=4° (C_{L_B}=0.31 C_{L_E}=0.32)

a=8° (C_{L_B}=0.63 C_{L_E}=0.65)

a=10° (C_{L_B}=0.75 C_{L_E}=0.77)

Percent chord

NACA
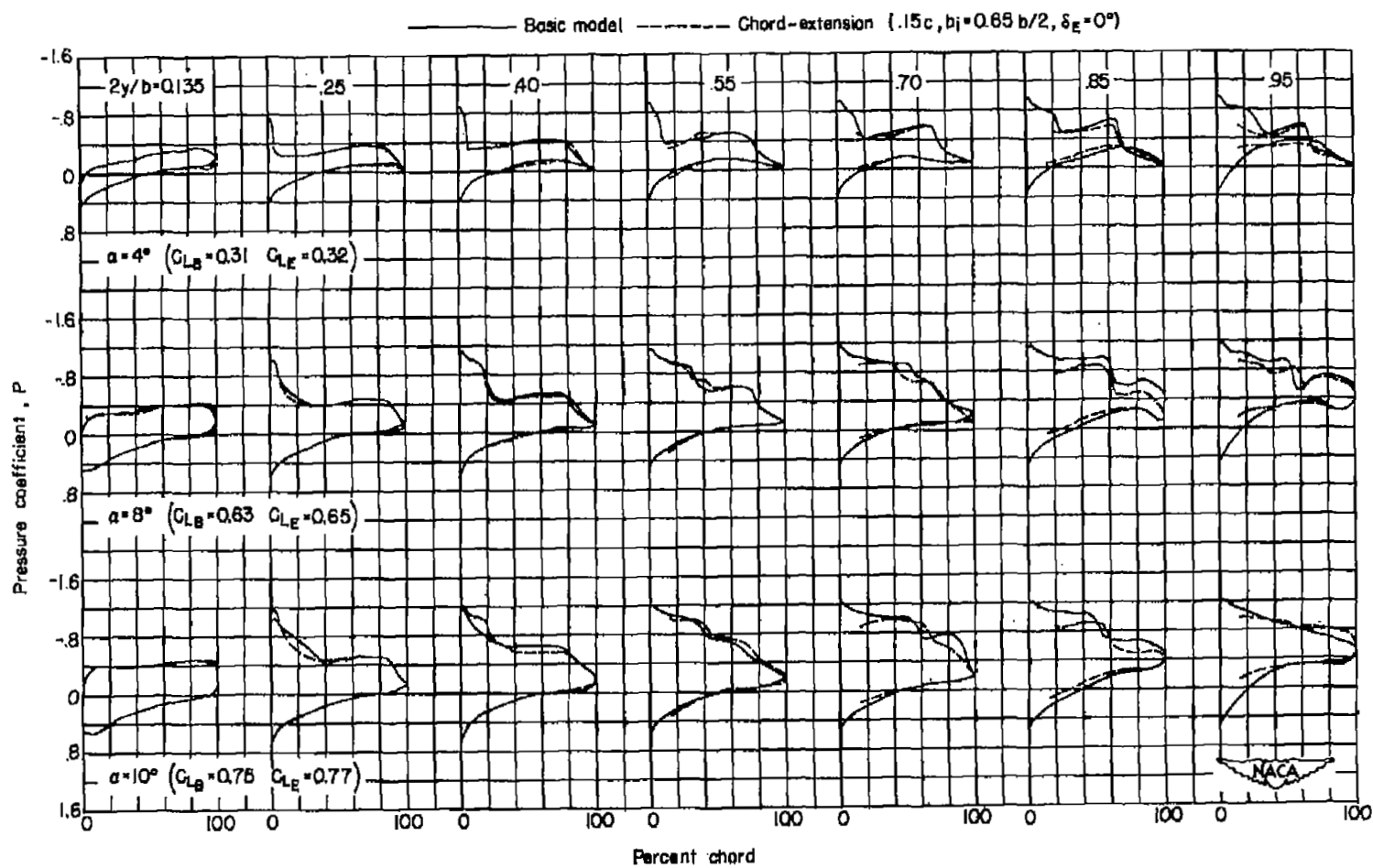
(g) M = 1.00; P$_{cr}$ = 0.

Figure 6.- Continued.

Basic model ———— Chord-extension (.15c, $b_i = 0.65\ b/2$, $\delta_E = 0°$)
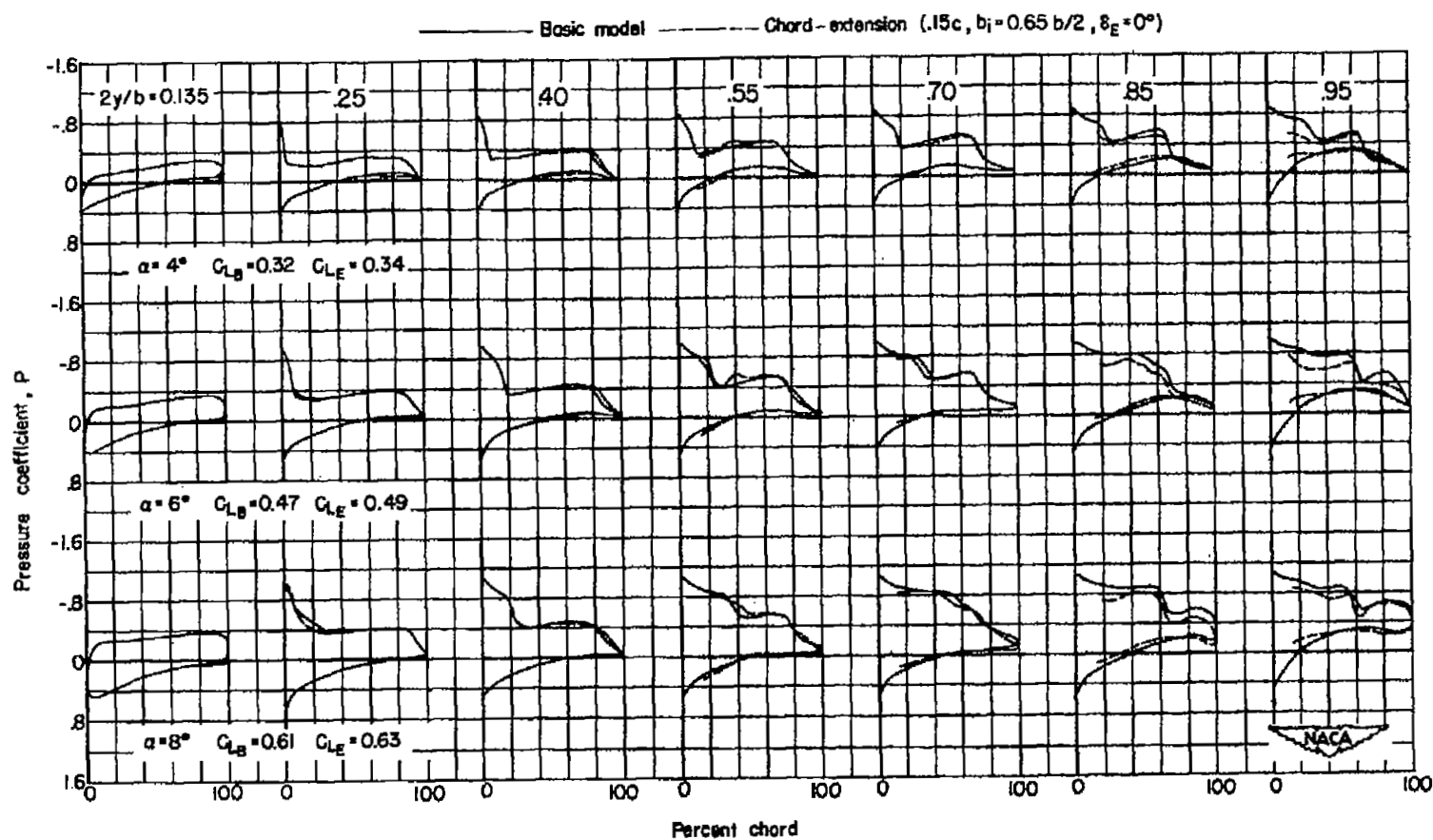
(h)   M ≈ 1.03; P_{cr} = 0.02.

Figure 6.- Concluded.

$\alpha = 4°$

$\alpha = 8°$

$\alpha = 12°$

$\alpha = 23.5°$

$\alpha = 18°$
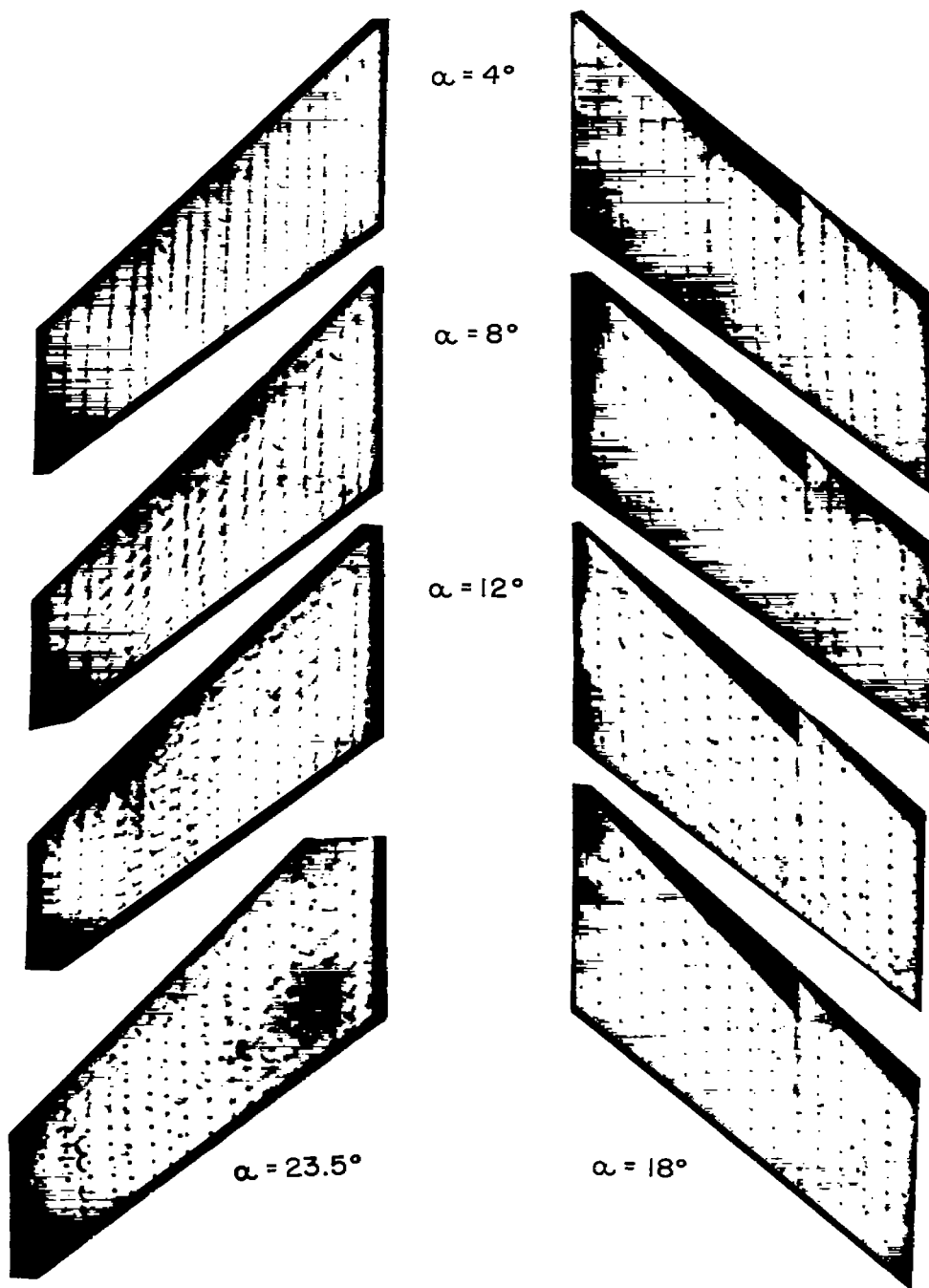
L-81191

Figure 7.- Tuft pictures showing flow over upper surface of wing (wing-
normal configuration) with and without chord-extension (0.20c,
$b_1 = 0.70b/2$, $\delta_E = 2.2°$) at a Mach number of 0.60.

M = 0.60

M = 0.80

M = 0.85
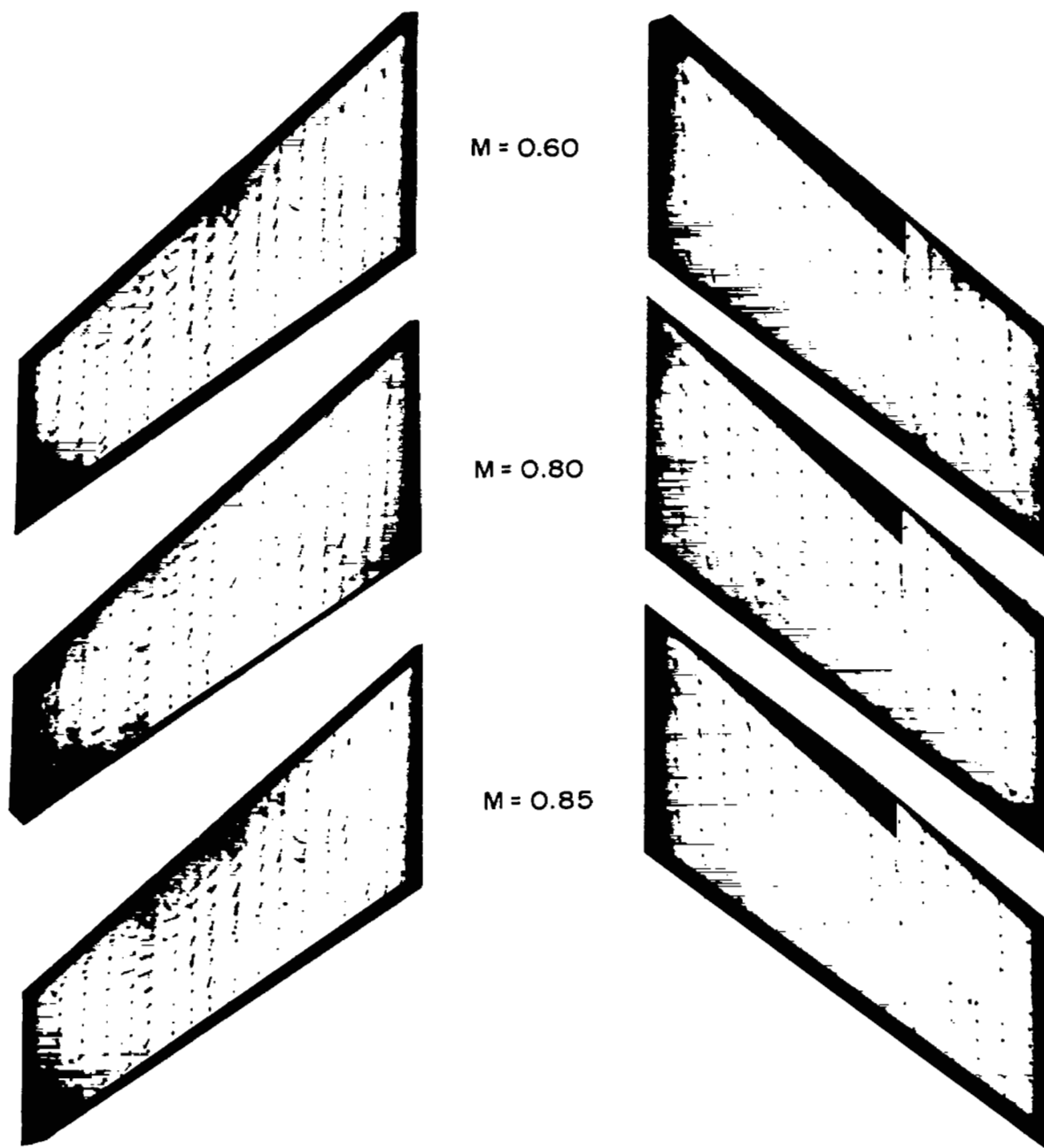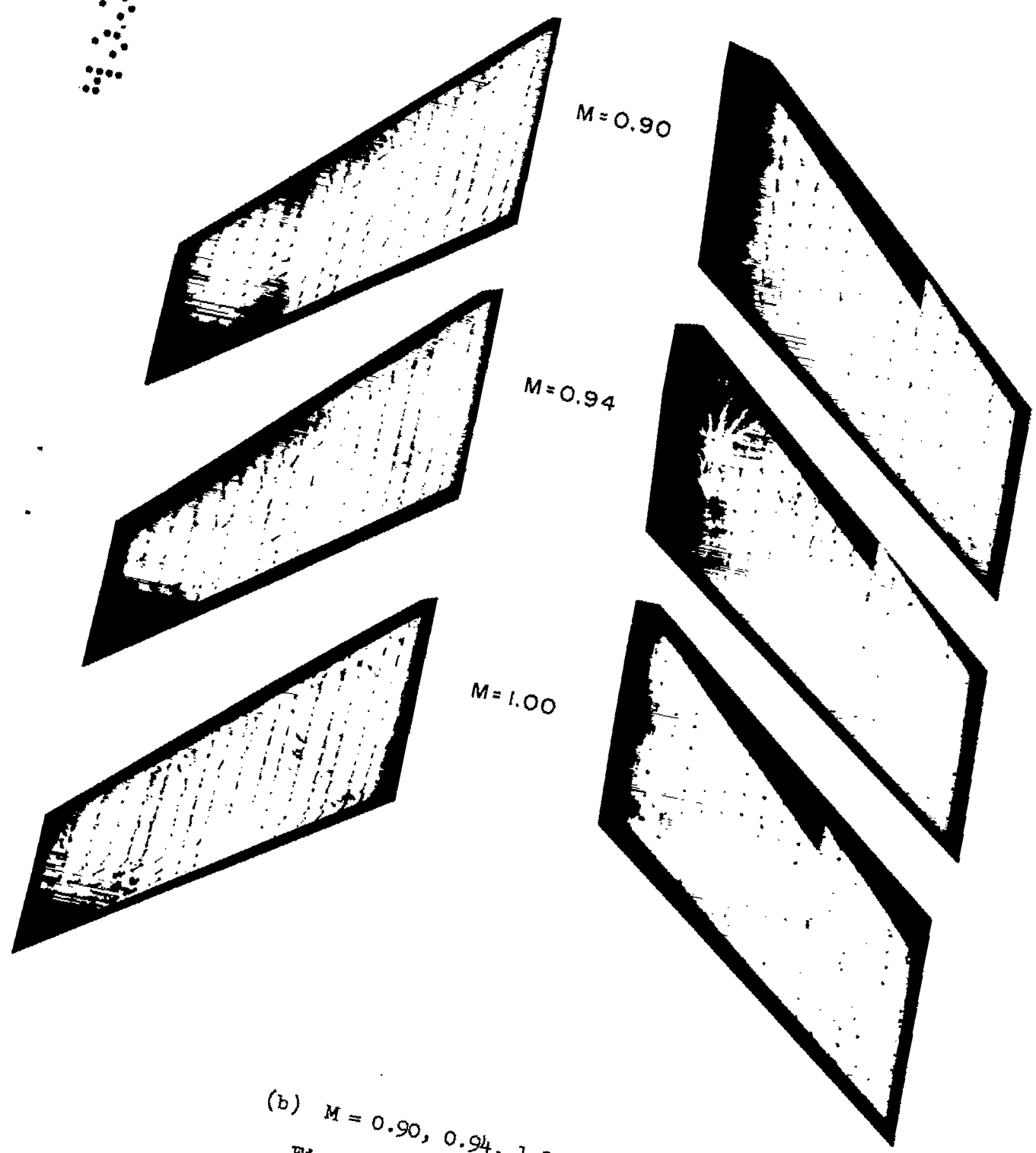
L-81192

(a)   M = 0.60, 0.80, 0.85.

Figure 8.- Tuft pictures showing flow over upper surface of wing (wing-
normal configuration) with and without chord-extension (0.20c,
$b_1 = 0.70b/2$, $\delta_E = 2.2^{\circ}$) at an angle of attack of 8°.

M = 0.90

M = 0.94

M = 1.00

L-81193

(b) M = 0.90, 0.94, 1.00.

Figure 8.- Concluded.
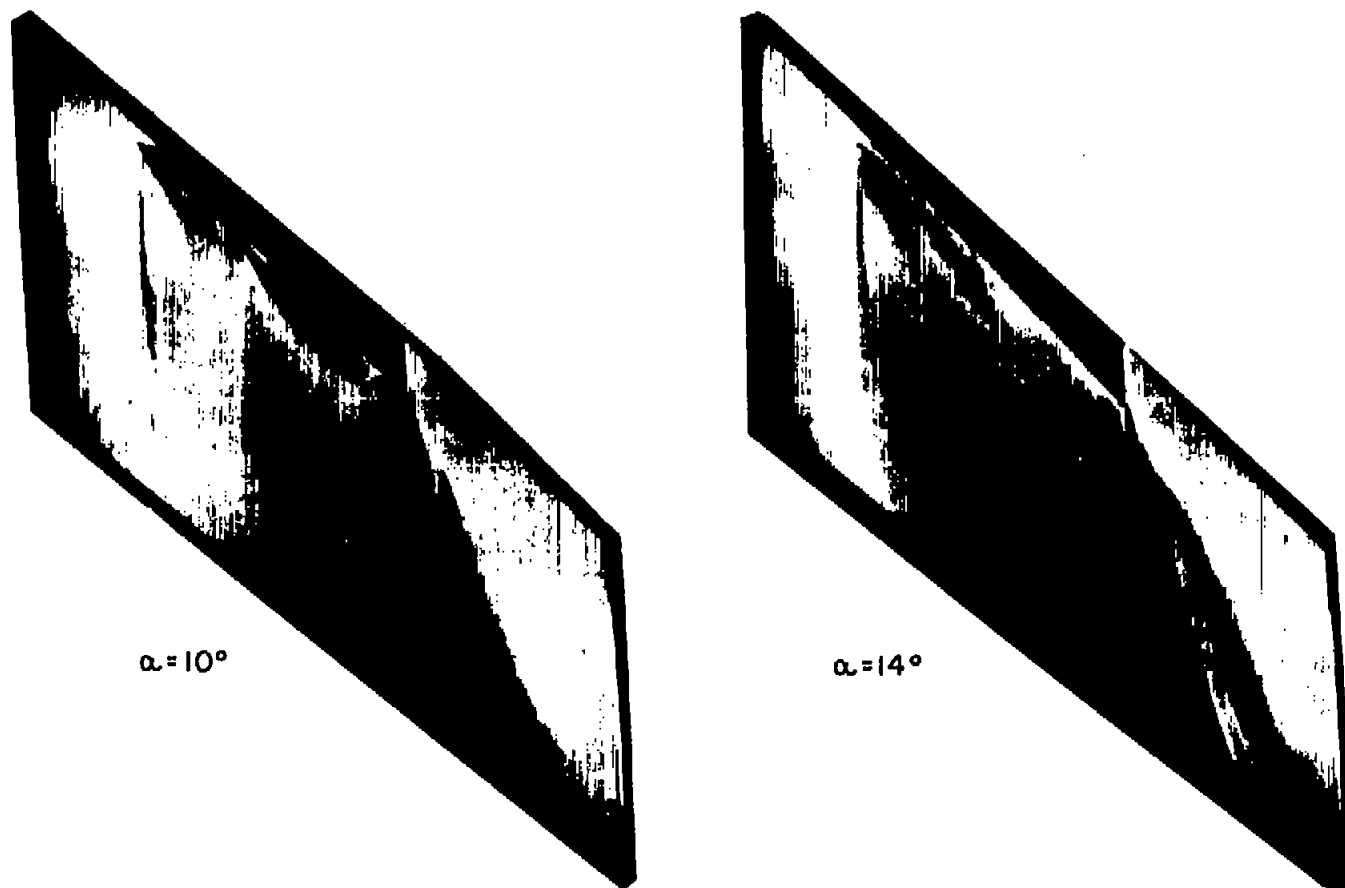
$\alpha = 10°$

$\alpha = 14°$

L-81186

Figure 9.- Ink-flow pictures showing flow over upper surface of wing (wing-aft configuration) with chord-extension (0.20c, $b_i = 0.70b/2$, $\delta_E = 0.4°$) at a Mach number of 0.60.

Trailing-edge shock

M=0.94 α=6°

Decelerating-flow
shock

Decelerating-flow shock

Leading-edge shocks

M=0.88 α=10°

M=0.94 α=10°

Trailing-edge shock
M=1.00 α=4°
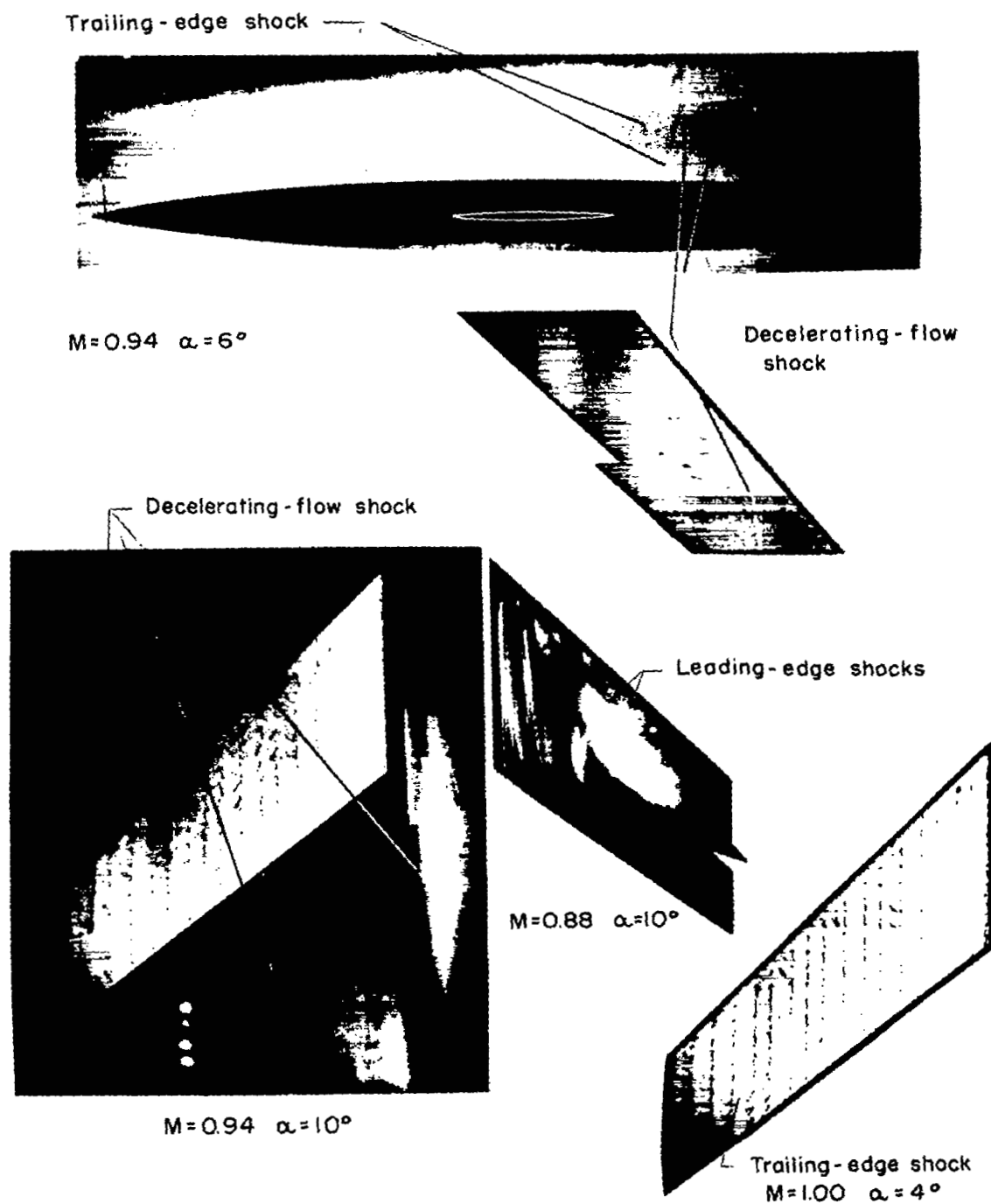
L-81194

Figure 10.- Examples of shocks that affect the flow over a sweptback
wing at transonic speeds.

Trailing-edge shock

Leading-edge shocks

Decelerating-flow
shock

NACA
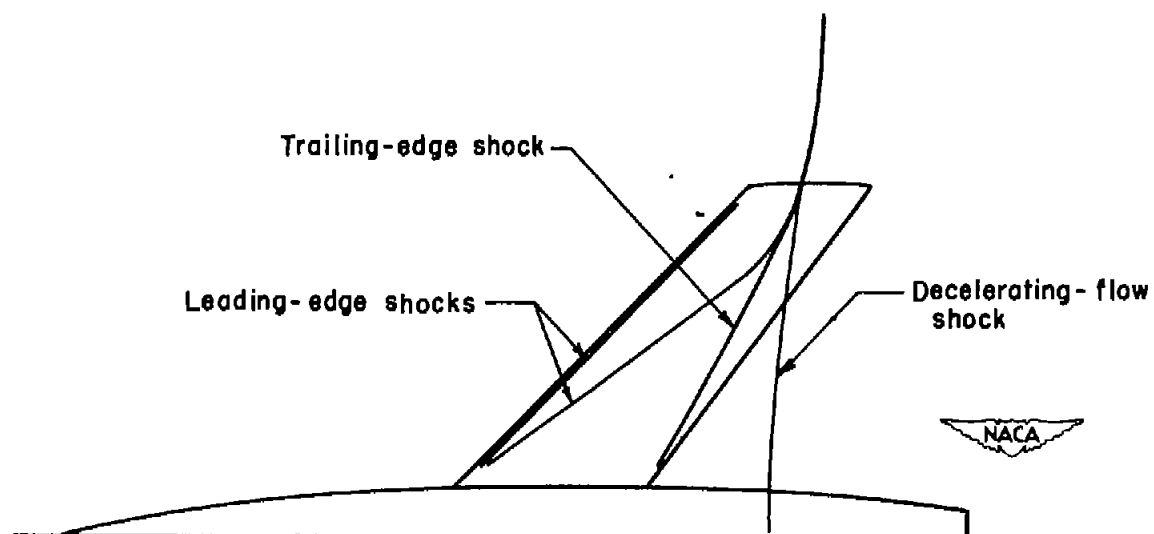
Figure 11.- Sketch showing typical shock pattern on basic wing.

α = 6°

α = 8°

α = 10°

α = 12°
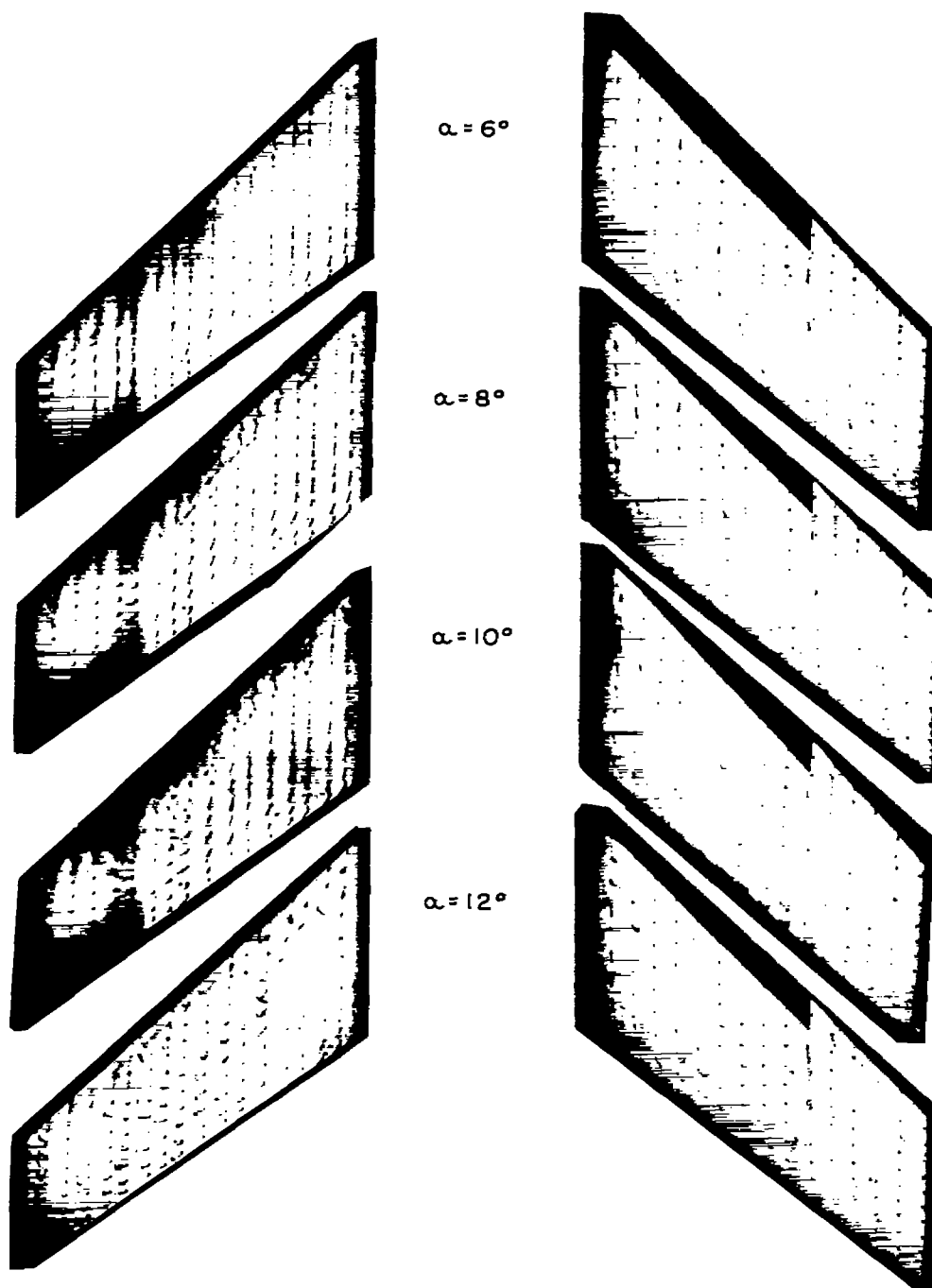
L-81195

Figure 12.- Tuft pictures showing flow over upper surface of wing (wing-normal configuration) with and without chord-extension (0.20c, $b_i = 0.70b/2$, $\delta_E = 2.2^o$) at a Mach number of about 0.90.
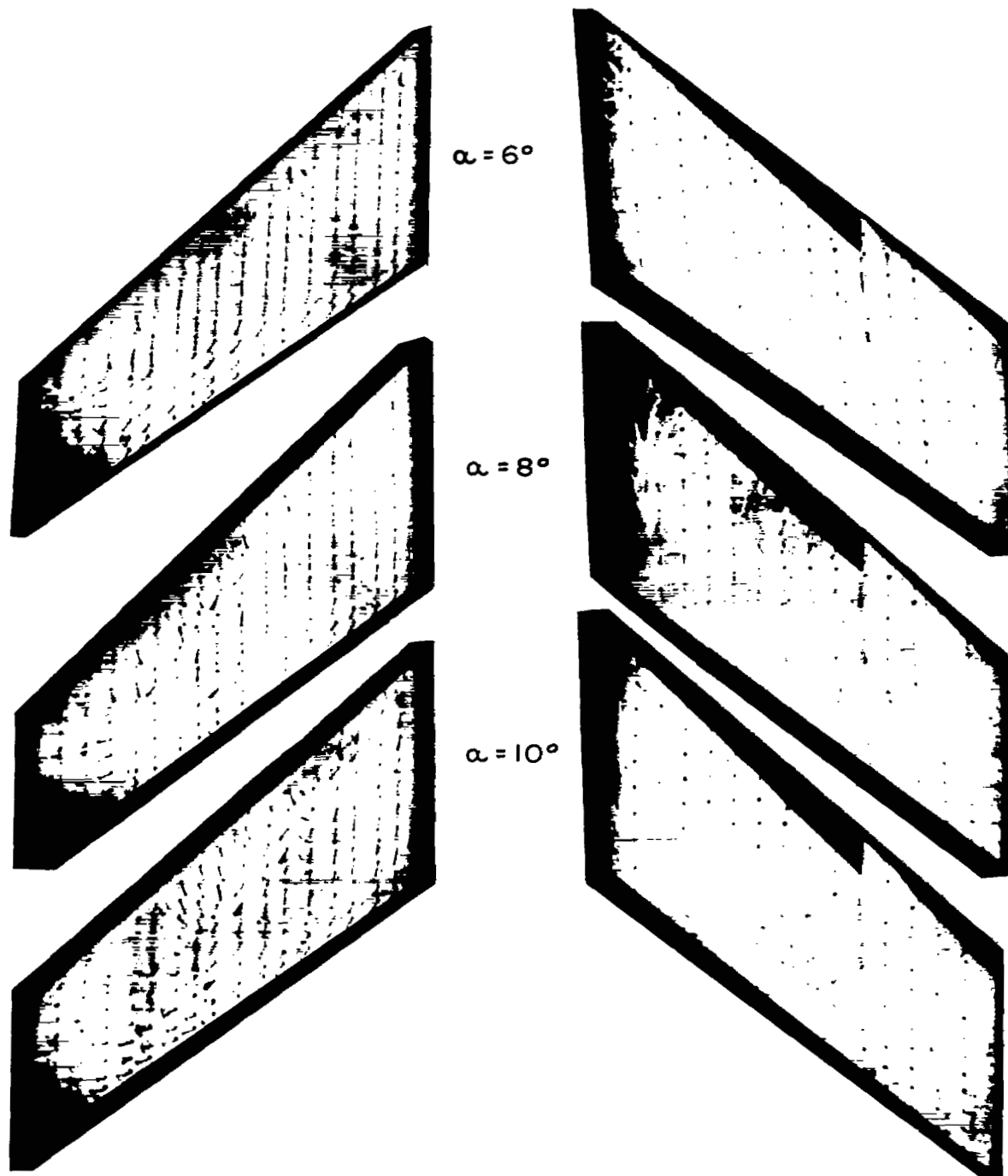
$\alpha = 6°$

$\alpha = 8°$

$\alpha = 10°$

L-81196

Figure 13.- Tuft pictures showing flow over upper surface of wing (wing-normal configuration) with and without chord-extension (0.20c, $b_1 = 0.70b/2$, $\delta_E = 2.2°$) at a Mach number of 0.94.
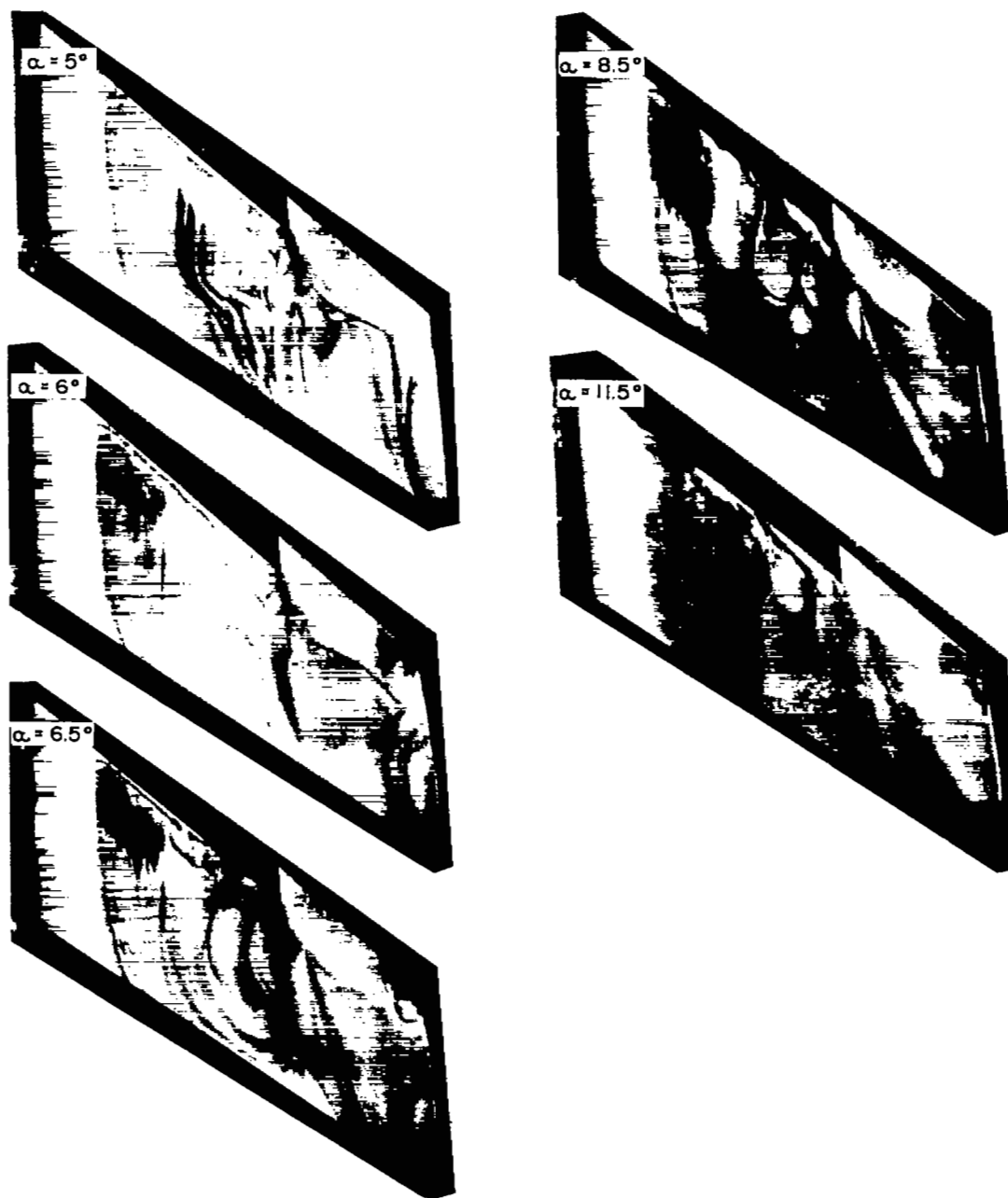
L-81187

Figure 14.- Ink-flow pictures showing flow over upper surface of wing
(wing-aft configuration) with chord-extension (0.20c, $b_1 = 0.70b/2$,
$\delta_E = 0.4°$) at a Mach number of 0.90.